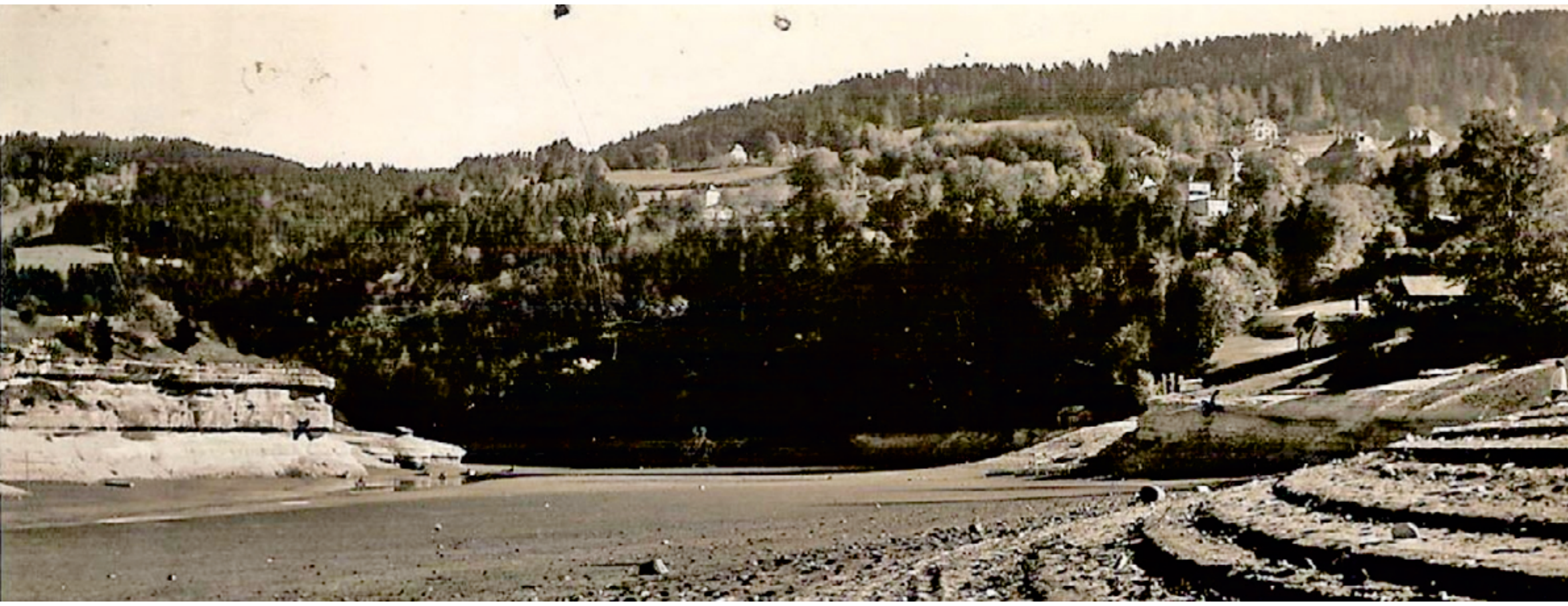

Hot and dry summers in Switzerland

Causes and impacts of the record summers 1947, 2003, and 2018

GEOGRAPHICA BERNENSIA

Hot and dry summers in Switzerland

Causes and impacts of the record summers 1947, 2003, and 2018

Translations:

Stefan Brönnimann, Noemi Imfeld, Peter Stucki

Layout:

Alexander Hermann

Bibliographic Data:

Imfeld, N., P. Stucki, S. Brönnimann, S. Bader, M. Bürgi, P. Calanca, S. Gubler, A. Holzkämper, L. Hövel, F. A. Isotta, C. Kestenholz, S. Kotlarski, A. Mastai, S. U. Nussbaumer, C. C. Raible, M. Röthlisberger, S. C. Scherrer, K. Staub, A. M. Vicedo-Cabrera, M.-M. Vogel, K. Wehrli, T. Wohlgemuth and H. J. Zumbühl (2022). Hot and dry summers in Switzerland. Causes and impacts of the record summers 1947, 2003, and 2018, Geographica Bernensia, G98, 33 p., doi:10.4480/GB2022.G98.03.

Translations:
German (doi:10.4480/GB2022.G98.01)

French (doi:10.4480/GB2022.G98.02)

Affiliations

Stephan Bader

Climate Division
Federal Office of Meteorology and Climatology, MeteoSwiss

Stefan Brönnimann

Institute of Geography, University of Bern
Oeschger Centre for Climate Change Research, University of Bern

Matthias Bürgi

Swiss Federal Institute for Forest, Snow and Landscape Research WSL
Institute of Geography, University of Bern

Pierluigi Calanca

Climate and Agriculture Group, Agroscope

Stefanie Gubler

Climate Division
Federal Office of Meteorology and Climatology, MeteoSwiss

Laura Hövel

Institute of Geography, University of Bern
Oeschger Centre for Climate Change Research, University of Bern

Annelie Holzkämper

Climate and Agriculture Group, Agroscope
Oeschger Centre for Climate Change Research, University of Bern

Noemi Imfeld

Institute of Geography, University of Bern
Oeschger Centre for Climate Change Research, University of Bern

Francesco A. Isotta

Climate Division
Federal Office of Meteorology and Climatology, MeteoSwiss

Christoph Kestenholz

Institute of Social and Preventive Medicine, University of Bern
Oeschger Centre for Climate Change Research, University of Bern

Sven Kotlarski

Climate Division
Federal Office of Meteorology and Climatology, MeteoSwiss

Alina Mastai

Institute for Atmospheric and Climate Science, ETH Zurich

Samuel U. Nussbaumer

Institute of Geography, University of Zurich

Christoph C. Raible

Physics Institute, University of Bern
Oeschger Centre for Climate Change Research, University of Bern

Matthias Röthlisberger

Institute for Atmospheric and Climate Science, ETH Zurich

Simon C. Scherrer

Climate Division
Federal Office of Meteorology and Climatology, MeteoSwiss

Kaspar Staub

Institute of Evolutionary Medicine, University of Zurich
Institute of History, University of Bern

Peter Stucki

Institute of Geography, University of Bern
Oeschger Centre for Climate Change Research, University of Bern

Ana M. Vicedo-Cabrera

Institute of Social and Preventive Medicine, University of Bern
Oeschger Centre for Climate Change Research, University of Bern

Martha-Marie Vogel

Man and the Biosphere (MAB) Programme, UNESCO, Paris

Kathrin Wehrli

Climate Division
Federal Office of Meteorology and Climatology, MeteoSwiss
Center for Climate Systems Modeling C2SM, ETH Zurich

Thomas Wohlgemuth

Swiss Federal Institute for Forest, Snow and Landscape Research WSL

Heinz J. Zumbühl

Institute of Geography, University of Bern

Content

Memorable summers

Do you remember the summer of 2018? A dry phase began as early as April and lasted until September. In many regions of Switzerland, hardly more than 50 percent of the normal amount of precipitation fell during this time. Rivers, even lakes, dried up, such as the Lac des Brenets on the Swiss-French border (Fig. 1.1). At the same time, temperatures remained consistently high, and it was the warmest summer half-year since measurements began in 1864. In addition, a strong heatwave struck Switzerland in late July/early August (Fig. 1.2).

Fig. 1.1: *The dried-up Lac des Brenets on 18 September 2018 (© Keystone).*

An event report by the Federal Office for the Environment[1] highlights the effects on agriculture and forests, water bodies and glaciers, health, and air pollution. It soon became clear that this summer was only a glimpse at summers to come, when in the fall of 2018 the new CH2018 climate scenarios for Switzerland, prepared by the Federal Office of Meteorology and Climatology, MeteoSwiss, ETH Zurich, the University of Bern, and ProClim, were presented to the public.[2] However, the summer of 2018 was not only extreme in Switzerland; almost the entire northern hemisphere was affected: North America, Europe, and Asia. This is unusual, and it shows the influence of man-made greenhouse gases, without which such an event can no longer be explained.[3]

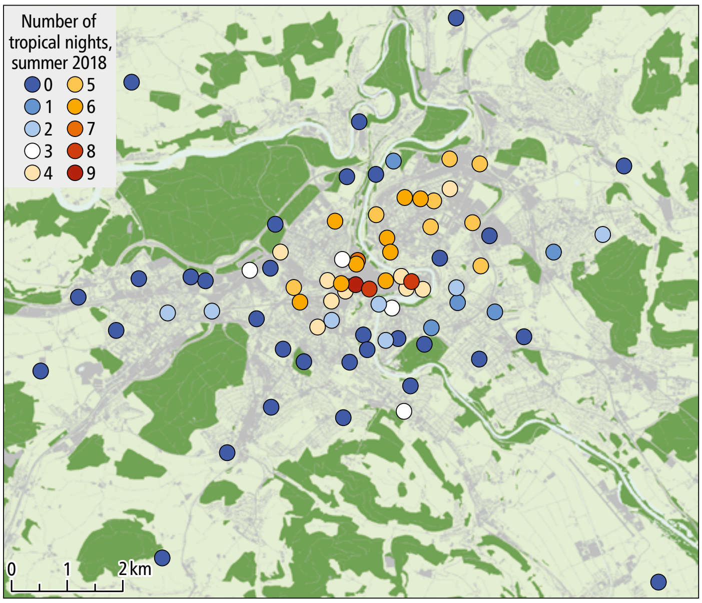

Fig. 1.2: *The urban heat island effect exacerbates the already unbearable heat. In the measurement network of the Geographical Institute of the University of Bern, eight to nine tropical nights (nights when the temperature does not fall below 20 °C) were recorded in the city centre in the summer of 2018, while only zero to two were recorded in the surrounding areas.[13]*

Yet the last similarly extreme summer occurred only three years earlier. In 2015, Switzerland was also affected by drought and heat, gardens turned brown, and the heat was intense.[4] Already then, the Federal Office for the Environment prepared an event report, and comparisons were made with the record heat summer of 2003. Comparisons have also been made, and continue to be made, with another event: The heat and drought summer of 1947 (see box).

Exactly 75 years ago – some may still remember – Central Europe was hit by a record heatwave. At many locations in Central Europe, the temperature records of that summer[5] were only broken in 2003 or during the heatwaves of 2019. In Switzerland, too, some of the records set in 1947 were held until 2003 (although it should be noted that the measurements taken at that time were probably influenced by radiation and were therefore possibly too high). At the same time, the summer of 1947 was extremely dry in Switzerland,[6] just as dry as in 2018. Furthermore, 1947 was only the most remarkable in a whole series of dry summers around 1950. Agriculture was severely affected by the drought of 1947.[7] Forests suffered[8,9] and Alpine glaciers melted.[10] Rivers dried up (see box; Lac des Brenets also dried up in 1947), with consequences for energy production and transport. Interestingly, there were also warnings of climate change: of desertification triggered by deforestation.[11] Especially in Germany, which was still suffering from the consequences of the Second World War, the summer of 1947, had devastating effects. Impressive audio and visual documents document the situation in Switzerland and Germany.[12]

How do such dry summers come about? How does a heatwave develop? What are the consequences for people and society, for agriculture and forestry, for our glaciers? And what do we have to prepare for in the future? This booklet provides answers to these questions.[13] Short chapters on individual topics shed light on the processes, comparing the summers of 2018, 2015, 2003, and 1947. At the same time, we look at the increasing frequency and intensity of heat summers over the past 150 years and venture a look into the future.

In the first chapter, the summer of 1947 is placed in the context of available measurements since 1864. It is shown how exceptionally warm and dry the summer of 1947 was and how it fits into the summers of recent decades that have been strongly influenced by man-made climate change. In the second chapter, we take a closer look at atmospheric dynamics, the processes that lead to heatwaves, and what it takes to develop a heatwave into a heat summer.[14] On a somewhat larger scale, the third chapter explains how the ocean and large-scale atmospheric processes influence the occurrence of heatwaves in Europe. In the fourth chapter, we consider how drought and decreasing soil moisture can amplify heatwaves. We then turn to the consequences of such extreme years for our natural environment. What are the consequences of extreme heat and drought for agriculture, and how did the population suffer in 1947 compared to today? What are the consequences of heat and drought for forests and what influence do other factors have on the amount of damaged wood caused by such extreme years? How did the heat translate into melting glaciers? In the ninth chapter, we address how people suffer directly from the heat and how this can be inferred from excess mortality.[15] Last but not least, we take a trip into the future: How often will we experience such extreme summers as 1947, 2003, 2015, or 2018 in the future?

The booklet shows the consequences of hot and dry summers for humans and nature – consequences that need to be managed. For there is no doubt that the intensity and frequency of hot summers will increase. The booklet also shows in an exemplary way that already 75 years ago very different areas of nature and society were affected: Health, water management, agriculture, forests, and glaciers. All in all, the summer of 1947 was one of the most momentous climate events of the 20th century. We can learn from this event. One might argue that the situation was quite different back then. The transition to a post-war economy was still underway, the vulnerability of society was much greater, and the dependence on agriculture stronger. This is certainly true. However, it is precisely because of this that we can learn lessons today. Even today and in the future, which will be shaped by man-made climate change, there will be societies in vulnerable situations, in phases of political transition or economic dependence. There are also more vulnerable people in our society whom we must protect as best we can from the consequences of future heatwaves.

This booklet was only possible thanks to the spontaneous willingness of the authors to contribute. The production of the booklet was supported by the Sebastiana Foundation, the Swiss Academy of Sciences (the Atmospheric Chemistry and Physics commission and the Association Suisse de Géographie), and the Oeschger Centre for Climate Research. The booklet is published simultaneously in three languages.

A film was also produced for the booklet, which is available on Youtube: [www.giub.unibe.ch/1947]

***Fig. 1.3:** Front page of an article in the "Schweizer Illustrierte" of 27. August 1947 about the consequences of "the great drought" in the summer of 1947, especially for agriculture. Courtesy of the Ringier Axel Springer Publishing House*

Eyewitness accounts of the hot and dry summer of 1947

How should we imagine the summer of 1947? What consequences did it have for people and animals? What was on people's minds at the time, how did they experience the summer? For this booklet, we interviewed various people who experienced the summer of 1947.

"The drought began in April. But because it had been quite wet before, the grass didn't suffer much, and we could still make hay. Then it got worse and worse," recalls Rudolf Bachmann, who grew up as a farmer's son on the Bantiger. The drought was soon joined by other difficulties: Cock chafer grubs damaged bushes and trees. There was little fodder for the cattle and the slaughterhouses were full. The heat was almost unbearable, and it lasted well into autumn.

"People were happy to ride bicycles, wore light clothes, and sought cooling in the baths of Bern," says Hulda Eggenberg. "At that time, however, women's and men's compartments were still separate." As a dressmaker in an haute couture shop in Bern, a big problem for her was not to sweat on her fingers.

"My father bought an American Goodridge garden hose in the summer of 1947. That was something special back then," Christian Röthlisberger recounts. The 1947 vintage was a good one, he adds. It was still praised long after, even though the quantity produced was small.

The hot summer of 1947 followed the years of privation during the war. In Germany, therefore, the summer of 1947 had a particularly dramatic impact. In Switzerland, the consequences were less severe. However, it was followed by another year of privation, which was soon followed by another year of drought in 1949. Several of the people interviewed compared the summer of 1947 with that of 2018 – and thus agree with many of the scientific contributions in this issue. The interviews conducted for this issue – about 1947 and other heatwaves and other climate anomalies – are compiled in a film (see left).

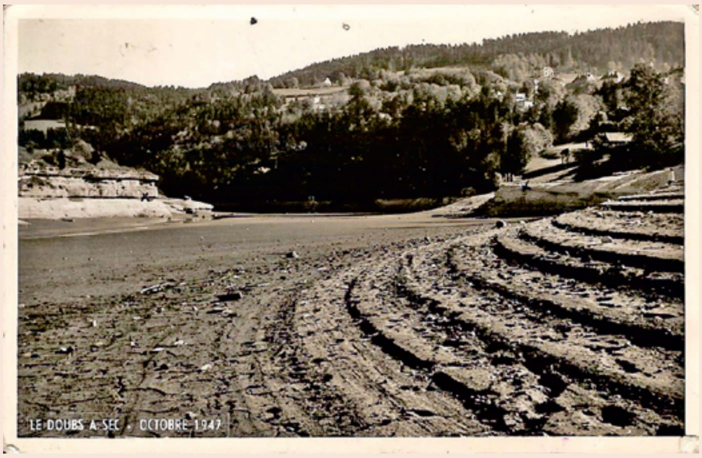

***Fig. 1.4:** The dried-up Lac des Brenets in the summer of 1947 (Pascal Huguenin, Pontarlier).*

The summer of 1947 in the context of climate change

The heat and drought in the summer half-year of 1947 were unique, especially in the context of that period. The occurrence of five heatwaves from May to September, combined with a massive drought on the Central Plateau, is unprecedented in the measurement series to this day. 1947 is still one of the warmest summer half-years to date and is still the driest since 1864 in north-western Switzerland and the central Swiss plateau. However, temperature and heat in the summer half-year have increased sharply in recent decades due to man-made climate change. A normal summer half-year today is only slightly cooler than in 1947. Dry summers have also become noticeably more frequent in recent decades.

Climate change is in full swing. In Switzerland, the decade from 2011 to 2020 was already around 2.5 °C warmer than the pre-industrial period from 1871 to 1900.[16] The consequences are manifold: glaciers are melting, there is less snow, precipitation and the hydrological cycle are changing, mass movements are increasing and ecosystems are in danger.[17] Here, we place the very exceptional summer half-year 1947[5,18,19] in the light of the now almost 160 year long history of continual measurements and in the light of the summer heat and drought events of the last twenty years, which have been strongly influenced by climate change.

Temperatures and heat

The time series of average summer temperatures across Switzerland shows the impressive warming over the last 160 years (Fig. 2.1a).[20] Today, summer half-years are usually more than 2 °C warmer than the pre-industrial average from 1871 to 1900. Extreme summer half-years are 2.5 to more than 3.5 °C warmer. The warm phase at the end of the 1940s is also noticeable in Fig. 2.1a. It is mainly characterised by the three warm summer half-years in 1945, 1947, and 1949. While 1945 and 1949 were just under 2 °C warmer than the pre-industrial average, 1947 stands out with a deviation of 3 °C. At that time, with a mean of just under 12 °C, it was around 1.2 °C warmer than ever before in the measurement period (in Geneva and Basel since at least 1753 and 1755 respectively) and thus an extremely rare event.[19,21] After the heat summers of 2018[22] and 2003[23,24] 1947 is still the third warmest summer half-year. However, summer half-years today have become massively warmer due to man-made climate change. For example, there are twelve summer half-years after the year 2000 that were warmer than 11 °C, whereas this value was never reached in the 137 years from 1864 to 2000, except in 1947. An average summer half-year today is only 0.8 °C cooler than in 1947.

Low precipitation and drought

In 1947, the Swiss Plateau was also affected by an extreme lack of precipitation and a "regionally catastrophic" drought.[7,18,19,25] To place the drought in context, we calculate an average precipitation value for the Swiss Plateau from the four long, homogeneous measurement series Basel/Binningen, Bern/Zollikofen, Genève/Cointrin, and Zürich/Fluntern. The series of Swiss Plateau precipitation in the summer half-year is characterised by large year-to-year fluctuations (Fig. 2.1b). In contrast to temperature, it shows no clear long-term trend. 1947 is the summer half-year with the least precipitation in the 158-year series of measurements from 1864 to 2021, with only 52 percent of the mean precipitation of the period from 1871 to 1900. The years 1865, 1870, 1911, and 1949 are also very low in precipitation, all with 63 to 65 percent of the pre-industrial precipitation total. The recent heat summers of 2018 and 2003 were higher in precipitation, at 69 and 70 percent respectively.

However, drought is more than a lack of precipitation. Since evaporating water is no longer available to vegetation, increasing evaporation plays a decisive role in water availability and the manifestation of a drought.[22] A simple measure that takes evaporation into account is the climatological water balance (precipitation minus potential evaporation, Fig. 2.1c). With an average water deficit of 330 mm, 1947 is clearly the driest summer half-year in the 158-year measurement series. At first glance, the water balance series is similar to the precipitation series, but there are important differences. The low-precipitation years of the last decades move up in the water balance ranking, while earlier years lose ground. The hot summers of 2018 and 2003, for example, are among the three driest, with a water deficit of around 260 mm, while the low-precipitation summer half-years of 1911 and 1870 (ranked 3 and 4) no longer make it into the driest five. Since the year 2000, dry summer half-years have become more frequent: in seven years, a water deficit of more than 100 mm was recorded. Further studies show that over the last forty years, slightly decreasing precipitation and increasing evaporation have contributed to the observed accumulation of dry summer half-years in roughly equal measure.[26]

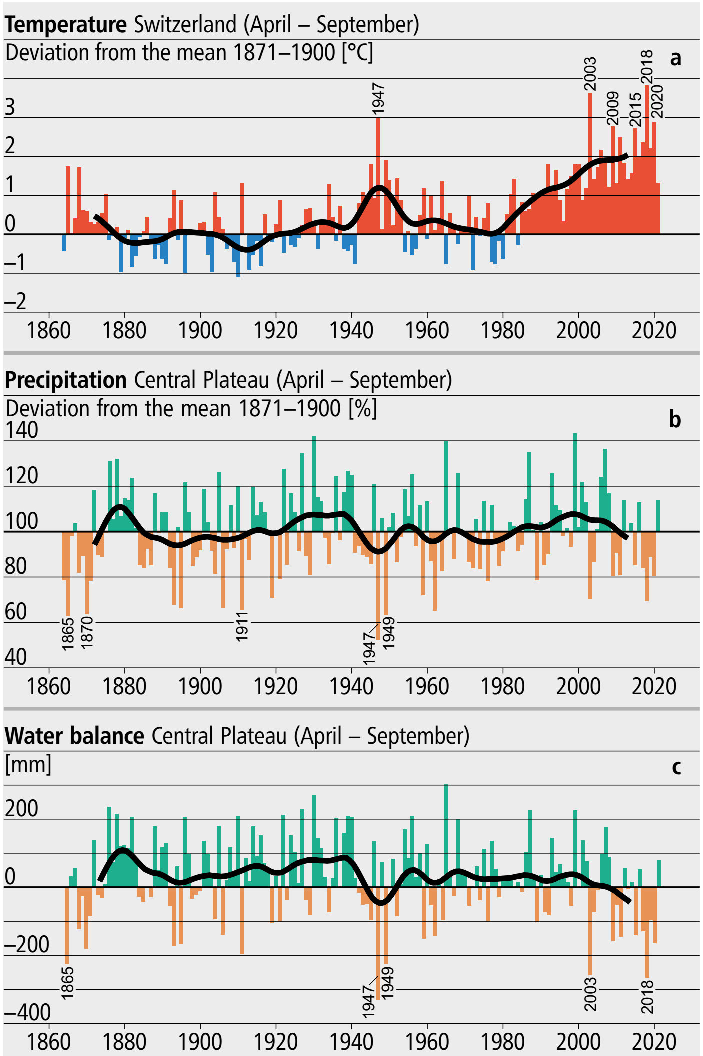

***Fig. 2.1:** a) Development of Swiss temperature (deviation in °C)[20], b) of Central Plateau precipitation (deviation in percent) and c) of the climatological water balance (precipitation minus potential evaporation) in the Central Plateau (in millimetres of water) in the summer half-year (April to September) since 1864. The deviations (a and b) refer to the pre-industrial average from 1871 to 1900. The five or six warmest/lowest precipitation/driest summer half-years are marked respectively. The black curve shows the smoothed development (20-year Gaussian filter). Central Plateau: an average of four stations (see text). Data: MeteoSwiss*

Regional characteristics of heat and drought

In terms of mean temperature, 1947 is the third warmest summer half-year after 2018 and 2003. Can it also keep up with the hottest summers in recent times in terms of heat? For this purpose, we look at the frequency of the heat in the form of the number of hot days (Fig. 2.2a) at the four stations Basel/Binningen, Bern/Zollikofen, Genève/Cointrin, and Zürich/Fluntern. With 26 to 43 hot days, depending on the station, most of 1947 can keep up with the recent heat summers or even exceed them in some cases. Only Genève/Cointrin, with 50 hot days in 2003, registered significantly more hot days than in 1947, where 34 hot days were recorded. A similar picture emerges for heat intensity. The 1947 values between 33.9 and 36.2 °C were only significantly exceeded in 2003 at all stations and in 2015 in Genève/Cointrin. However, further studies show that long-lasting heatwaves have become significantly more frequent in recent decades.[21] For example, ten-day heatwaves with a mean daily maximum temperature of 30 °C or more in western Switzerland now follow each other at short intervals of one to two years. Other regions also witness an increasing frequency of long heatwaves.

Drought can vary greatly from region to region. This is shown by the evaluation of the water balance at the four stations on the Central Plateau individually (Fig. 2.2b). In Basel/Binningen a water deficit of over 460 mm was recorded in 1947. In Bern/Zollikofen and Zürich/Fluntern, likewise, 1947 is the driest summer half-year to date, with deficits of 330 and 285 mm, respectively. In Genève/Cointrin, in contrast, 1947 is only the fourth driest summer half-year. In parts of eastern Switzerland, 2018 was significantly drier than 1947.[22] In 1947, drought particularly affected north-western Switzerland and the central Swiss Plateau (see also Fig. 2.1), where 1947 is still the driest summer half-year since systematic measurements began in 1864.

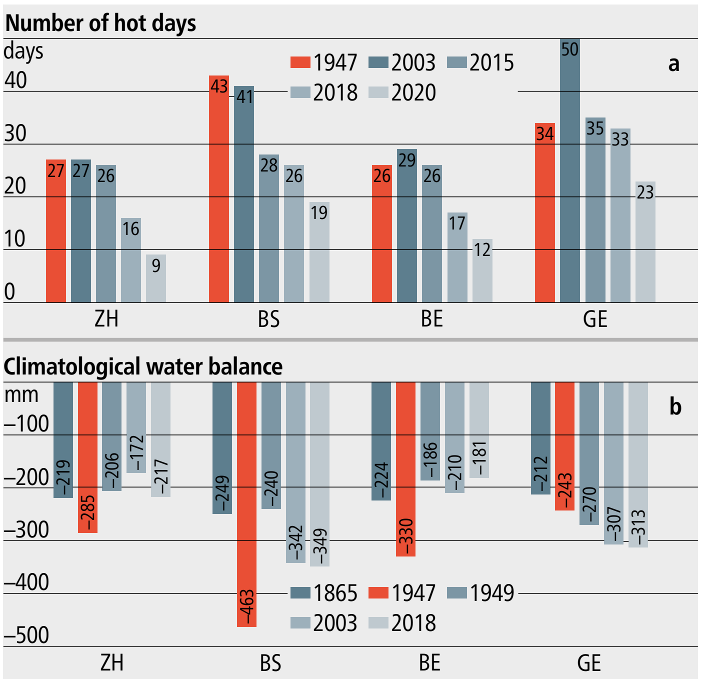

Fig. 2.2: a) number of hot days for the five pronounced heat summer half-years 1947 (red), 2003 (dark blue), 2015 (blue), 2018 (medium blue), and 2020 (light blue), and b) climatological water balance (precipitation minus potential evaporation in millimetres) for the five very dry summer half-years 1865 (dark blue), 1947 (red), 1949 (blue), 2003 (medium blue) and 2018 (light blue) at the four stations Zürich/Fluntern (ZH), Basel/Binningen (BS), Bern/Zollikofen (BE) and Genève/Cointrin (GE).

The exceptional summer half-year of 1947

The summer half-year of 1947 was characterised by "much sunshine, high temperatures, little cloud cover, and precipitation".[18] There was a remarkable sequence – unique in the instrumental record since 1864 – of five heatwaves, spread over the whole summer half-year (see Fig. 2.3).[5] The first occurred from the end of May to the beginning of June. A short second one followed at the end of June. The third, hottest and longest heatwave of 14 days lasted from 22 July to 4 August and reached a mean daily maximum temperature of 35.0 °C for the example of Basel. In mid-August, there was a fourth heatwave lasting about eight days, followed by a fifth heatwave lasting nine days from 11 September. For the summer half-year, there was a heat surplus of 2.5 to 3.5 °C in places compared to the pre-industrial average of 1871 to 1900, with the largest deviations in the western and central parts of Switzerland.

In addition to the warmth, the summer half-year of 1947 was characterised by a marked lack of precipitation on the northern side of the Alps.[18,19,27] On the Central Plateau, only 300 to 400 mm of precipitation fell from April to September (Fig. 2.4), which corresponds to about half the usual amount of precipitation. In a band from Lake Neuchâtel to Schaffhausen precipitation was less than 300 mm, in the Basel region even only around 200 mm.[28] The lack of precipitation, combined with the high temperatures, led to a pronounced drought "of great rarity and impressiveness". The consequences included massive failures in agriculture[25,28] (see p. 16), water shortages at the municipal water suppliers, and losses in electricity production.[19] In the following chapter we will analyse this weather situation and why it led to heat and drought.

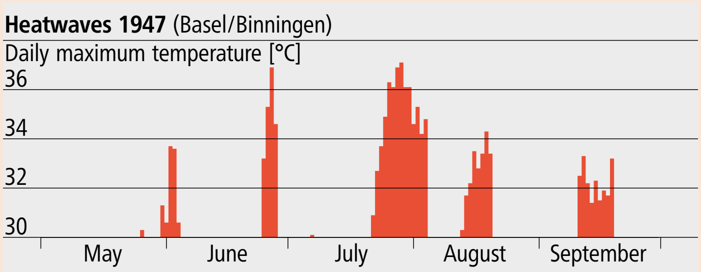

Fig. 2.3: The five distinct heatwaves from May to September 1947 using the example of the Basel/Binningen station. The temperatures of the days with a daily maximum temperature greater than or equal to 30 °C are marked in red.

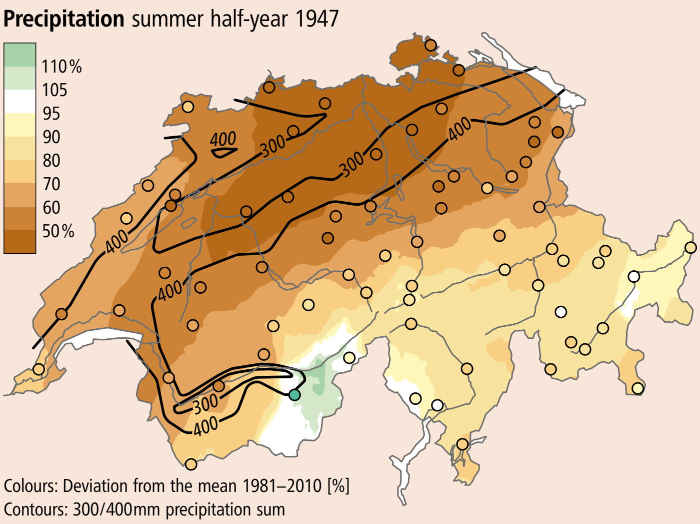

Fig. 2.4: Reconstructed precipitation maps for the summer half-year 1947.[29] Deviations from the 1981 to 2010 mean are shown in percent (colours), as well as the isolines of the precipitation amounts 300 and 400 mm (bold black lines).

Atmospheric dynamics: From a hot air parcel to a very hot summer

In this article, we shed light on the formation of heatwaves on various spatial and temporal scales. Starting with an individual air parcel, we discuss how an air parcel changes its temperature, in which weather systems heatwaves develop, and how individual heatwaves can evolve into an entire extreme summer. In addition, we summarise the most important synoptic features of the summer 1947.

How does air change its temperature?

Our journey through the spatial and temporal scales of heatwaves begins with an individual air parcel, for example, the air that was located about 100 metres above Bern at 2 p.m. on August 13, 2003, and was around 30 °C warm at that time. To understand how this air parcel could become so warm, we can examine the air parcels' path on its journey through the atmosphere. This path is called "trajectory." Along its trajectory, an air parcels' temperature changes on the one hand due to pressure changes resulting from sinking (i.e., subsiding) or ascending motion, which results in compression or expansion of the air parcel (so-called "adiabatic" temperature changes). On the other hand, its temperature is affected by radiation, turbulence, or phase transformations of water (e.g. condensation of water vapour), which are referred to as "diabatic" temperature changes.

Figures 1a and b show this interplay of adiabatic and diabatic processes along the trajectory of the air parcel located over Bern at 2 p.m. on August 13, 2003 (colored trajectory in Fig. 3.1). On August 3, this air parcel was still at a pressure level of 600 hPa (about 4500 m a.s.l.) over the Atlantic and then subsided to 800 hPa over the eastern Atlantic and England until August 8. During this process, the air parcel warmed by 20 °C, whereby periods of strong subsidence were also associated with strong temperature increases (Fig. 3.1b). During the last three days prior to the arrival in Bern, the air parcel was located near the ground in the lowermost kilometre of the atmosphere. During this time, the temperature evolution decoupled from the pressure evolution, as diabatic processes started to strongly influence the temperature and the air parcel hardly moved vertically anymore. The jagged pattern in Figure 1b shows the classical diurnal cycle in temperature, arising from diabatic heating during the day and diabatic cooling at night by radiation, sensible heat fluxes, and turbulence.

During heatwaves in Central Europe, the near-surface air is heated both by subsidence and by diabatic processes.[30,31] Contrary to common notions, this heatwave air mostly approaches Central Europe from northwest to northeast and only in rare cases from the climatologically warmer southerly regions.[31] This is illustrated exemplarily by the trajectories of the air parcels that reached Bern between August 6 and 13, 2003, which mainly approached Switzerland from northeast and which were located over the Atlantic Ocean a few days before (Fig. 3.1a). In cases when air masses from southerly regions approach Central Europe, they usually ascend over the colder air in Central Europe and therefore often do not reach the surface at all. However, the relative importance of compression, diabatic processes, and the simple horizontal transport of warm air for heatwaves is still a subject of active research.

Synoptic scale – weather systems and heatwaves

Whether and where heatwaves develop is related to the synoptic-scale circulation (i.e., the large-scale circulation over several thousand kilometres) in the middle and upper troposphere (5000–12 000 m a.s.l.). At these heights is the jet stream, a band of strong westerly winds that undulates from west to east. These waves of the jet stream, the so-called "Rossby waves", steer and modulate the occurrence of high- and low-pressure areas and thereby determine to a large extent how the surface temperature changes. This relationship is illustrated in Fig. 3.2a–c, which show the jet stream at 300 hPa (wind vectors), surface temperature anomalies, and sea level pressure for three days at 12 UTC during the summer of 1947. The largest positive temperature anomalies in Western Europe at all time steps are found in the central and eastern part of a "ridge", which is the region where the jet stream describes

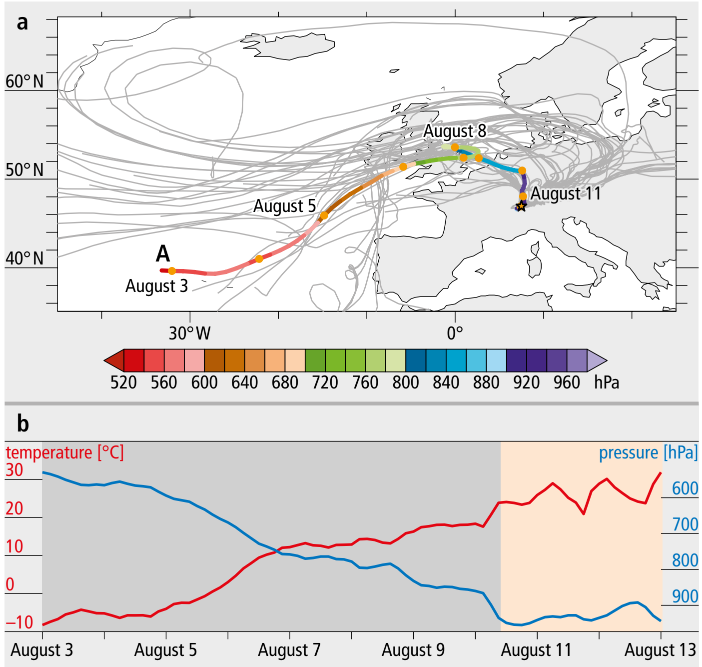

Fig. 3.1: *a) Trajectories of the air parcels arriving in Bern from 6 to 13 August 2003 at about 100 m above ground (in grey).[46,47] The trajectory of the air parcel with an arrival time of 2 p.m. local time on 13 August (the hottest day of the summer in Bern) is coloured by its pressure. b) Evolution of pressure (blue) and temperature (red) in air parcel A. Grey and orange shading in (b) indicate periods during which temperature changes in air parcel A were primarily adiabatic and diabatic, respectively.*

a poleward deflection. The negative temperature anomalies further east, however, are located below a "trough", i.e., below an equatorward deflection of the jet stream. Positive temperature anomalies occur in the central and eastern part of the ridge because there the air is descending near the surface and the middle troposphere and thereby heated adiabatically. This adiabatic warming leads to cloud-free skies, as cloud droplets and ice crystals evaporate or melt and sublimate during subsidence. The descending of the air thus also leads to stronger solar radiation, which diabatically warms the air near the surface.[32]

If a ridge is located over a region for a particularly long time, this typically favours the development of heatwaves, since the air near the surface can warm up over several days.[31-34] This often happens when the Rossby waves reach a particularly large amplitude (i.e., extension in a north-south direction), thereby reduce their phase speed and deform strongly[35] (this process is called Rossby wave breaking). Such ridges can remain stationary for days and sometimes even weeks (in these cases they are called "blocks" or "blocking high-pressure systems"), and shift the normal west-east propagation of low-pressure systems to the north or south.[36] In central and northern Europe, heatwaves occur mainly in association with blocks.[32] Also, during the heatwaves in the summer of 1947, several blocking high-pressure systems were located over Europe, however at different positions (green lines in Fig. 3.2a–c).

From a heatwave to a very hot summer

Individual heatwaves are thus strongly related to particular synoptic-scale weather systems, but how do individual heatwaves become an entire extremely hot summer? Answering this question in detail is difficult because at any location of the globe only very few seasonal heat extremes occurred since weather data have been collected con-

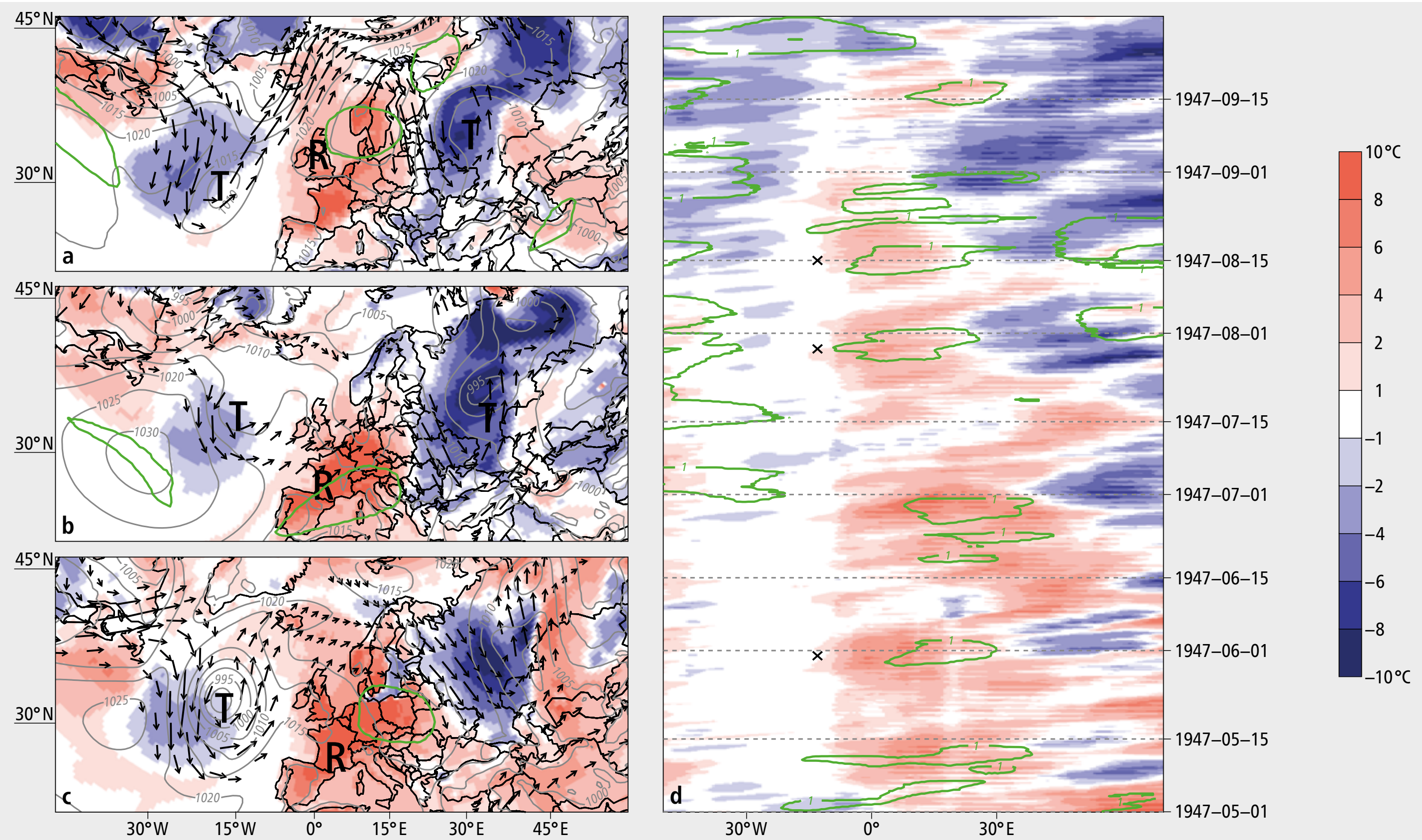

Fig. 3.2: *a–c) Meteorological situation during three heat days on 31 May (a), 29 July (b), and 15 August (c) 1947 at 2 p.m. local time. Temperature anomalies are calculated relative to the 1931 – 1960 daily climatology at 2 p.m. (shading). The jet stream is apparent from the vectors, which show the 300 hPa wind wherever its velocity exceeds 18 m/s. Surface pressure (in hPa) is shown as grey lines. Green lines show blocked areas[48], and troughs and ridges are labelled with T and R, respectively. d) Longitude-time plot of May to September 1947 hourly temperature anomalies averaged over 35°–65°N (shading) and blocks (green lines). The three crosses indicate the times for which maps are shown in the left column. The data are from the reanalysis 20crv3.[49]*

tinuously and reliably. However, it is clear that the duration and temporal organisation of heatwaves (and the weather systems responsible for them) play a key role. During the extremely hot summers of 2003 and 2018 in Europe, as well as 2010 in western Russia, several but also particularly long-lasting heatwaves occurred,[37-41] which were associated with long-lasting blocks, especially during the summer of 2010 in western Russia.[40,42] Such a long-lasting block is typically repeatedly re-enforced by ridges that form to the west of the block and are absorbed by the block.[36,43,44] In addition, it is known that the recurrent formation of ridges in the same location (even without a block) can lead to particularly long-lasting heatwaves.[45] The temporally clustered occurrence of blocks and ridges is influenced by so-called teleconnections, climatic connections between widely separated areas. These modulate the triggering, propagation, and breaking of Rossby waves, thus influencing the frequency of midlatitude blocks and ridges (see p. 12). Heat summers over land also usually occur in conjunction with drought whereby heat and drought mutually reinforce each other through land-atmosphere feedbacks.

A summer with many blocks over Europe

Between May and September 1947 several, as well as unusually strong heatwaves occurred in succession. The temperature anomalies averaged between 35°N and 65°N (Fig. 3.2d) were almost continuously strongly positive between May and September and interrupted only by short episodes with average temperatures. Blocks were repeatedly present over Europe throughout the summer – depending on the area, their frequency in the summer of 1947 was up to three times greater than the average for these months in the period 1931 – 1960 (Fig. 3.3a; the term "frequency" here refers to the fraction of the 1947 summer during which blocks occurred at each grid point). The frequent blocking situations in 1947 can be explained by the fact that a resemblant large-scale flow patterns with a ridge over Europe (Fig. 3.2a – c) established in a recurrent manner. The recurrence of similar flow patterns had led to a particularly large number of different blocks, depending on the region up to four blocks more than in the average of the years 1931 – 1960 (Fig. 3.3b), which corresponds roughly to a doubling of the number of blocks compared to climatology. This indicates that especially the temporal organisation of these blocks (i.e., their recurrence in a relatively short period) may have played a pivotal role in generating the extremely hot summer of 1947.

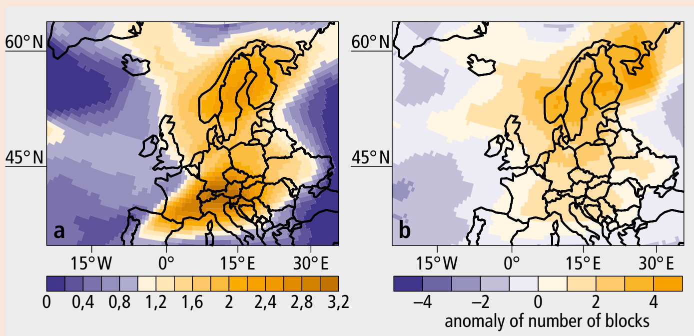

Fig. 3.3: *a) ratio of the frequency of blocks in summer 1947 (May to September) and the May to September climatology from 1931 – 1960; b) anomaly of number of blocks relative to the 1931 – 1960 climatology [same months as in (a)]. The data are from the reanalysis 20crv3.[49]*

Large-scale and oceanic factors of heatwaves in Central Europe

Oceans and the large-scale atmospheric circulation have a significant influence on European heatwaves and the associated weather systems. Both anomalously cold and anomalously warm sea surface temperatures in the North Atlantic are related to the occurrence of heatwaves in Central Europe. In the following article, we discuss how these sea surface temperatures and the upper tropospheric atmospheric circulation influence the occurrence of heatwaves in Central Europe.

Atmospheric-Oceanic interaction

How do changes in sea surface temperature affect the atmosphere? Experiments with climate models show that a negative sea surface temperature anomaly (colder sea surface temperatures than usual) leads to a positive pressure anomaly, i.e., a high-pressure area in the overlying lower troposphere. At the same time, a negative pressure anomaly, i.e., a low-pressure area, develops in the upper troposphere (7000–12 000 m a.s.l.).[50] However, this general reaction of the atmosphere is modified in the mid-latitudes by the storm activity. Storm activity refers to the westerly wind circulation prevailing in the mid-latitudes and the low-pressure areas that move from west to east. Theoretical studies show that due to this storm activity, an altitude-independent and stationary low-pressure area forms downstream, i.e., east of the cold sea temperatures (Fig. 4.1a).[51] In the case of a negative sea surface temperature anomaly in the northern North Atlantic, a stationary low-pressure area forms off the British Isles. In this low-pressure area, cold air from the polar regions is transported southward on its western flank, supporting the negative sea surface temperature anomaly (Fig. 4.1b). Thus, we see a self-reinforcing interaction. A ridge of high-pressure forms to the east of the low-pressure area. Thus, this process represents one way in which high-pressure ridges form over Europe, which can then trigger heatwaves in Central Europe.[52] How heatwaves can form in high-pressure ridges is further described on page 10. A case study of the 2015 heatwave identified a strong negative sea surface temperature anomaly in the northern North Atlantic as a key driver, but similar negative temperature anomalies associated with heatwaves also occur in other years.[53] The authors find a strong negative sea surface temperature anomaly in the North Atlantic influencing the atmospheric circulation such that the strong wind band in the middle and upper troposphere (5000–12 000 m a.s.l.) becomes fixed, allowing a ridge of high pressure to form over Europe.

Another process described in the literature is the link between the Atlantic Multi-decadal Variability (AMV), a sea surface temperature variation in the North Atlantic, and heatwaves in Europe.[54] Multi-decadal variation here refers to a fluctuation in sea surface temperature that persists over several decades. In this case, the authors considered the sea surface temperature in the central-western North Atlantic to be important, rather than that in the northern North Atlantic.

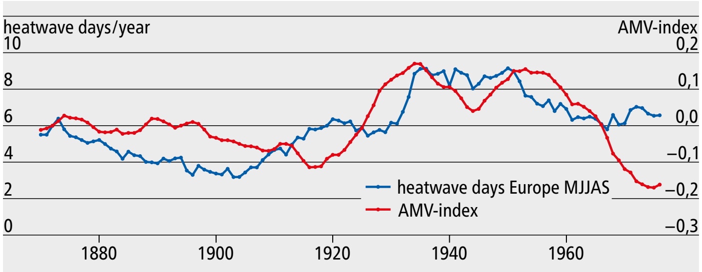

Fig. 4.2: *Heatwave days over Europe (climatology 1850–1900) and Atlantic Multidecadal Variability index[59] (both rolling average over 10 years). The temperature data are from the reanalysis 20crv3.[49]*

They describe a relationship between warmer-than-usual sea surface temperatures (a positive AMV anomaly) and an increased number of heatwave days over Central Europe (Fig. 4.2). This positive sea surface temperature anomaly in the northwest Atlantic causes heat flux from the ocean to the atmosphere, resulting in a negative pressure anomaly east of the heat source. The negative pressure anomaly can then trigger the process described above, leading to heat and drought in Central Europe. Figure 4.3 confirms this relationship statistically, that is, we see a positive correlation of sea surface temperature in the central-western North Atlantic with heatwave days over Europe, while a negative correlation is found northeast of it.

Thus, we see that both processes described, one starting from a sea surface temperature anomaly in the northern North Atlantic and one in the central-western North Atlantic, can lead to heatwaves and droughts. However, the statistical analyses also show that we cannot determine which of the processes plays the dominant role.

Influence of sea ice cover

In addition to the influence of the sea surface temperature, the decrease of the sea ice cover and the snow cover of Eurasia is also associated with an increase of heatwaves in Europe.[55] A weakening of the meridional, i.e., the north-south temperature gradient in the North Atlantic and over Eurasia is found to be responsible for a decrease in the storm activity in the mid-latitudes and a stronger meandering of the strong wind band in the middle and upper troposphere (5000–12 000 m a.s.l.). A decrease in storm activity means that fewer

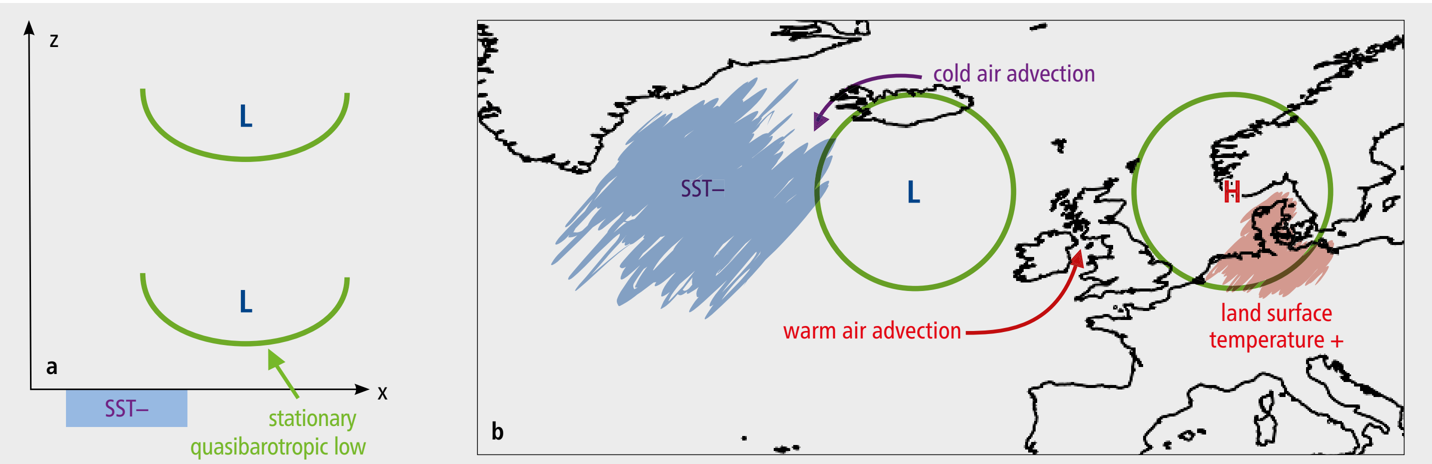

Fig. 4.1: *Schematics: a) influence of a negative sea surface temperature anomaly on the vertical air pressure distribution and b) horizontal distribution of sea surface temperature and air pressure with indicated transport of cold and warm air masses. b) illustrates the self-reinforcing interaction between ocean and atmosphere.*

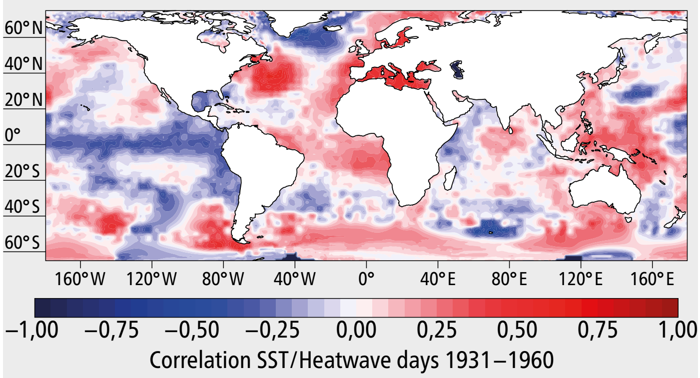

Fig. 4.3: *Correlation between the number of heatwave days (climatology 1850–1900 representative for the preindustrial period) over Europe (between 10°W to 40°E, 30 to 75°N) and sea surface temperature (May–September). Sea surface temperatures are from HadISST.*[60]

low-pressure areas pass over Europe. The decrease of storm activity and the stronger meandering of the strong wind band lead to a more frequent occurrence of blocks, the second phenomenon, which is related to heatwaves (see p. 10).

Amplification mechanisms in the upper troposphere

Another process that may favour the formation of heatwaves in Europe is based on an amplification mechanism in the upper troposphere, where the jet stream is located.[56] This mechanism considers a specific fraction of atmospheric waves, namely the stationary planetary waves in the upper troposphere (7000–12 000 m a.s.l.). These waves span the entire globe in a sequence of high- and low-pressure areas and usually have only a weak amplitude (i.e., a high-pressure area is only weakly pronounced). Under certain conditions, this stationary part of the atmospheric waves can be trapped in the waveguide of the mid-latitudes, which leads to resonance and thus to amplification of the waves (i.e., amplification of the high-pressure area). A waveguide can be thought of as a west-east oriented band, which guides the movement of individual waves from west to east. This amplification mechanism was examined concerning European heatwaves and it played an important role in the heatwave in 2018.[57] In particular, the division of the jet stream in the upper troposphere (7000–12 000 m.a.s.l.) into a northern and southern part is important for trapping the waves in the midlatitude waveguide and thus for amplifying the waves.[58] This was also the case in the 2018 heatwave, where a stationary high-pressure area had formed over Europe through this amplification process.[57]

A cold North Atlantic in the summer of 1947

The summer of 1947 was characterised by a strong cooling of the North Atlantic Ocean (Fig. 4.4). This cooling is comparable to the situation in 2015 in its strength of about 1.5 °C, in its position, and its extent (Fig. 4.5).[53] The cooling, in turn, appears to be related to a low-pressure area that was located downstreams of it (see Fig. 3.2). This similarity to 2015 suggests that the atmospheric-oceanic interaction described above must have played an important role in the formation of the heat summer in 1947 as well. The 1940s were also characterised by a positive phase of AMV (Fig. 4.2), which may also have contributed to increased drought and heat over Europe, as described above.

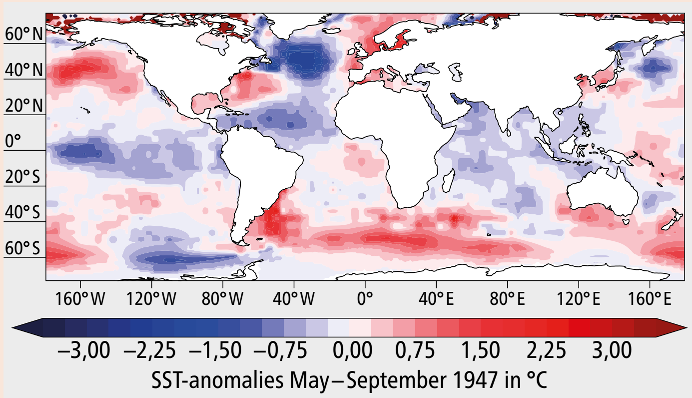

Fig. 4.4: *Sea surface temperature anomaly for the summer months of 1947 (May–September) compared to the 1931–1960 mean. Sea surface temperatures are from HadISST.*[60]

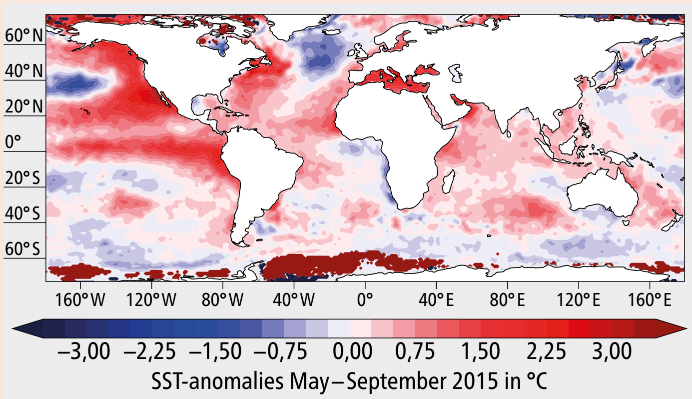

Fig. 4.5: *Sea surface temperature anomaly for the summer months of 2015 (May–September) compared to the 1991–2010 mean. Sea surface temperatures are from HadISST.*[60]

How drought-heat interactions drive hot summers in Europe

The summer heatwaves in 1947 in Switzerland were accompanied by a prolonged drought period that affected Central Europe from around 1945 to the early 1950s.[5] This concurrence of severe drought and heat also characterises the more recently experienced European summer heatwaves of 2003 and 2018 that were associated with devastating impacts on society, ecosystems, and the economy, such as heat-related deaths and losses in crop production.[3,61-63] This concurrence of droughts and heat will be explored in the following chapter.

Processes for the development of heatwaves

In Europe and the mid-latitudes, summer heatwaves are generally driven by atmospheric circulation anomalies, particularly stationary high-pressure systems (see p. 10), and can be reinforced by land-atmosphere feedbacks often related to the drying of the soils.[66,67] Soil moisture, the water content stored in the soil, can essentially affect the climate via the surface energy balance describing incoming and outgoing radiation at the surface. The net radiation at the surface can be described as the sum of the sensible heat flux, the latent heat flux, and the ground heat flux. The sensible heat flux describes the energy we can feel as temperature, whereas the latent heat flux describes the energy needed for the evaporation of water from the surface and the transpiration by plants and is also called evapotranspiration. Dry soils can lead to reduced latent heat flux, increased heating of the surface, warming and drying of the air, fewer clouds, and precipitation (Fig. 5.1). Regions can be characterised by dry, wet, and transitional soil moisture regimes, depending on the fraction of net radiation that is used for evapotranspiration called evaporative fraction.[68,69]

In the dry regime (e.g., desert regions) the soil moisture content is below the wilting point. Plants can thus no longer extract water from the soil and the evaporation is zero. Evapotranspiration is sensitive to soil moisture, but very small, as soils are dry. Such a regime is called a soil moisture-limited regime. In the transitional regime, the energy partitioning is sensitive to the soil moisture content and evaporation strongly depends on the availability of soil moisture. Therefore, regions in a transitional regime are hot spots for soil moisture-atmosphere feedbacks (see next section). Typical regions in the transitional regime are equatorial Africa and India. In the wet regime, the soil moisture content is above a critical soil moisture value; there is enough water available. Thus, net radiation controls evapotranspiration, and the regime is energy limited. Central and northern Europe including Switzerland are typically in a wet regime.[68,70,71] However, during the spring and summer months, these regions can enter a transitional regime where soil moisture-atmosphere feedbacks can be present.[71]

Soil moisture-atmosphere feedbacks

Soil moisture-atmosphere feedbacks can intensify summer heatwaves in Europe.[69,72] A decrease in soil moisture reduces the latent heat flux or evapotranspiration (Fig. 5.1 black arrow centre). Consequently, more energy is available for sensible heating which leads to an increase in near-surface temperatures (red arrows, top). The rising temperature increases the atmospheric water demand since warmer air can retain around 7 percent more water vapour per degree of warming (according to the Clausius-Clapeyron equation). This results in an increase in latent heat flux (red arrows, right) and an enhancement of the initial drying of the soils (red arrows, bottom) This feedback loop is called positive soil moisture-temperature feedback.

Soil moisture can also affect precipitation (Fig. 5.1, blue arrows). A decrease in soil moisture decreases the latent heat flux (Fig. 5.1 arrow centre). This can lead to a decrease in clouds and precipitation (blue arrows, top) and enhance the drying of the soils (blue arrows, bottom). This can be summarised as positive soil moisture-precipitation feedback. Such a positive coupling between latent heat flux and precipitation can be generally found in observations and climate model simulations on daily to monthly time scales.[73-77] The soil moisture-precipitation feedback can ultimately also influence hot temperatures as a precipitation deficit can be associated with a decrease in soil moisture which, in turn, can enhance sensible heat flux and near-surface temperature. Given that soil moisture is subject to change in a warming climate, this will influence future changes in hot extremes.

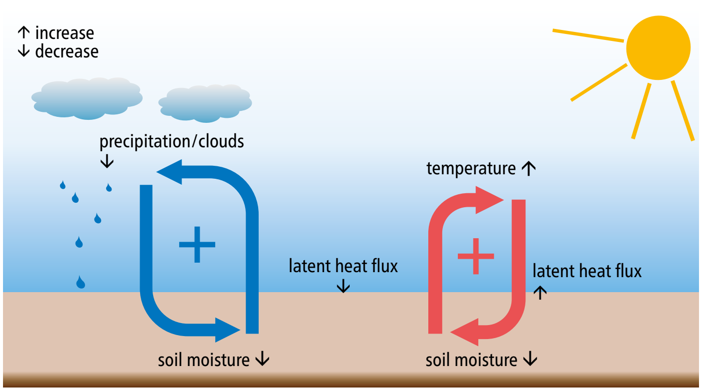

Fig. 5.1: *Positive soil moisture-temperature feedback (red) and positive soil moisture-precipitation feedback (blue) (adapted).[91]*

Future heatwaves

Climate projections suggest that European summer heatwaves will become longer, more frequent, and more severe during the 21st century with global warming.[64,72,78-80] Soil moisture-atmosphere feedbacks substantially contribute to this projected increase in temperature extremes in the mid-latitudes.[67,81,82] Projections show that the temperature on the hottest days of the year will increase by more than 9 °C in Central Europe at the end of the 21st century under a business-as-usual high-emission scenario with soil moisture feedbacks (Fig. 5.2a), whereas the warming is only around 5 °C for model simulations where soil moisture-temperature feedbacks are inhibited (Fig. 5.2b).[83] Soil moisture temperature-feedbacks can contribute up to 75 percent of the amplified warming of the hot extremes beyond global mean temperature.[83]

Thus, particularly in Europe, hot summers that are associated with severe droughts are projected to become more likely in a warming climate.[82,84] Also for Switzerland, climate model simulations project hotter and drier summers, with less precipitation and evapotranspiration and drier soils.[2] The number and temperatures on the hot days are projected to increase particularly in the densely populated urban areas at low elevations (see p. 24).

Exceptionally hot and dry summers 2003 and 2018

Switzerland experienced exceptionally hot and dry summers in recent decades, whereas 2003 ranked the hottest summer and 2018 the third hottest since 1864.[2] The 2003 summer heatwave represents one of the most severe natural disasters in Europe, with the number of excess deaths reaching tens of thousands and drastic losses to agricultural production.[61,85] The period from 1 to 13 August 2003 was the most extreme heat period in Switzerland since measurements started in 1864.[23] It was caused by a persistent atmospheric blocking over central and southern Europe[38,85,86] and preceded by a precipitation deficit in spring.[37] The stable weather with clear-sky conditions and strong radiative forcing in June and the heat accumulation in the boundary layer over several days enhanced the soil moisture depletion.[87] Thus soil moisture-atmosphere feedbacks significantly contributed to the hot temperatures observed during the 2003 summer heatwave.[66]

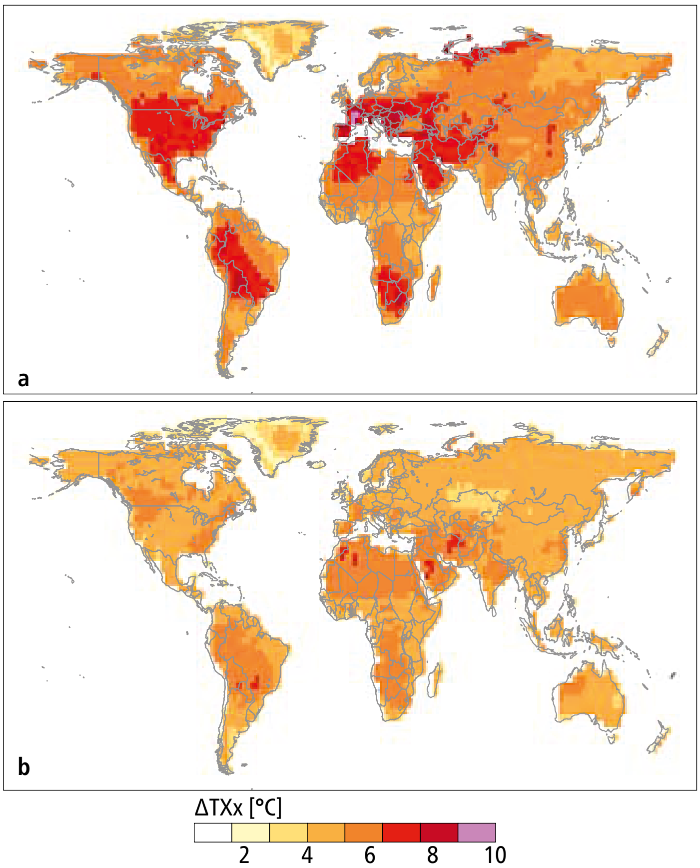

Fig. 5.2: *Projected changes of the temperature on the hottest day of the year (ΔTXx) between 2081–2100 and 1951–1970 for a) simulations with soil moisture-temperature feedbacks and b) simulations where soil moisture-temperature feedbacks are inhibited (right) (adapted).*[83]

In 2018 large parts of the mid-latitudes in the Northern Hemisphere concurrently experienced record-breaking heat extremes in spring and summer (May–August) associated with severe impacts (Fig. 5.3).[3] These concurrent heat events were unprecedented in terms of the total area affected by hot extremes for that period and would most certainly not have occurred without human-induced global warming. In central and northern Europe the 2018 summer was exceptionally hot and dry, and associated with forest fires in Scandinavia, heat stress, and agricultural production loss.[88,89] It has been very uncommon for the typically wet regime in northern Europe that soil moisture-temperature feedbacks amplify the warming.[89]

Thus, the 2018 summer highlights again the important role of soil moisture-atmosphere feedbacks for summer heatwaves. These unprecedented events may provide a foretaste of future heatwaves in Switzerland, given that the concurrence of drought and heat is projected to increase with higher levels of warming.[90]

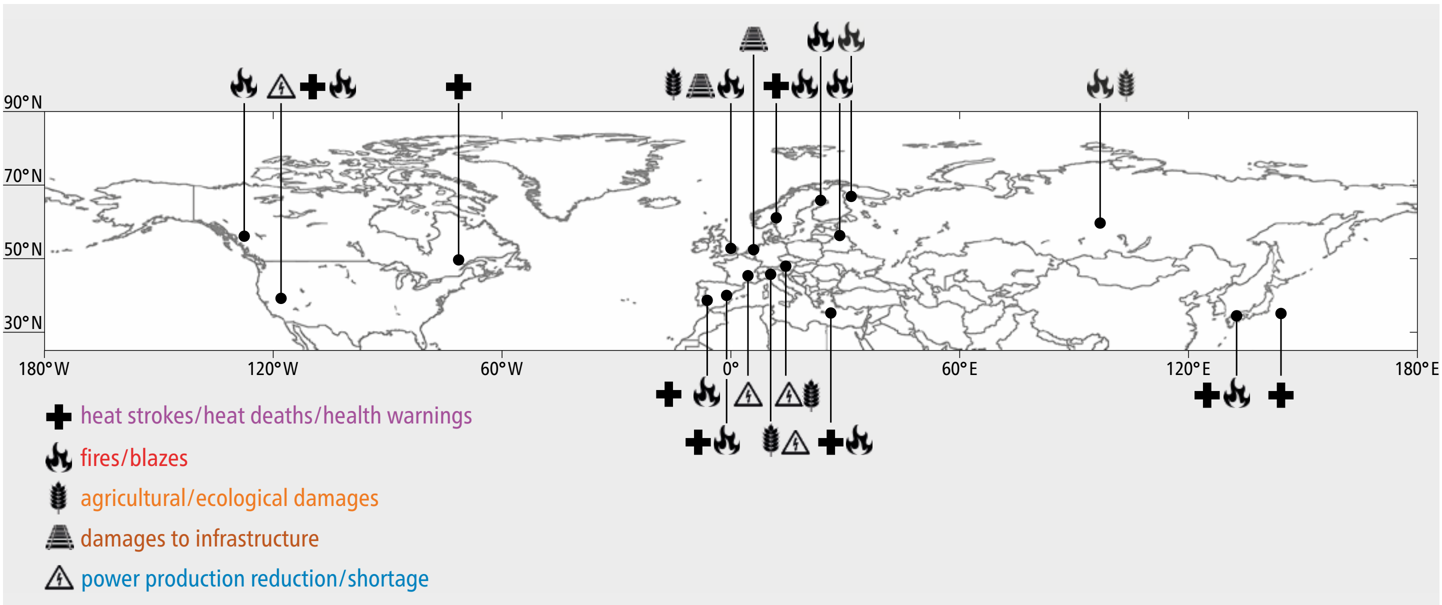

Fig. 5.3: *Reported 2018 heat-related impacts in newspaper articles (adapted).*[3]

Impact of the drought years 1947, 2003, and 2018 on agriculture

Droughts in the years 1947, 2003, and 2018 had severe impacts on grassland and livestock production. In arable farming, all three years showed both positive and negative yield anomalies, as the exact timing of the drought determines the impact on various crops. Overall, the Swiss population was much more affected by the 1947 drought than in recent extreme years because food security was substantially lower at that time.

Climatic constraints on crop production

In crop production, annual variations in yields are primarily determined by varying weather conditions during growing cycles. For a crop to achieve its highest possible yield, weather conditions must match the temperature and moisture demands of a certain crop during each growing season. Constraints from frost, drought, heat, radiation, and excessively low growing temperatures should be avoided. Hence, crop planting is routinely done such that the seasonal patterns of temperature and precipitation, on average and from experience, best suit the crop-specific needs. However, given the variability of weather, it is all but impossible to prevent certain climatic factors from having a yield-limiting effect in specific years. Thus, annual weather variability leads to varying yields of different crops, and climate variability and extremes can have diverse effects on specific crops.

Drought as a limiting factor

With only 300 mm in six months, less than 50 percent of the normal amount of water was available to vegetation in 1947. After a very wet March 1947, i.e., with a clear water surplus (Fig. 6.1), large precipitation deficits were recorded from April onwards. Coupled with above-average temperatures, this led to a long drought period (see p. 9). In northeastern Switzerland, the drought reached its first peak in June. In August, water balance deficits of 100 mm or more occurred throughout the Central Swiss Plateau, and it was not until October that this period of extreme drought ended.[92] The drought led to significant yield losses, as it persisted throughout the entire growing season in 1947. Lower yields were particularly evident in grassland farming, and grain yields were also below average in 1947 (Fig. 6.2). A similar pattern of yield anomalies was also observed for the extreme years 2003 and 2018, albeit with differences between crop species. This is explained in more detail below.

Shortage of forage

In grassland farming, the yield from the second cut of grass was particularly reduced in 1947. National yields were 10–13 percent below the 1920–1950 average, while yields of the first cut were less affected by adverse weather conditions (5–9 percent below the 1920–1950 average). Opportunities for imports were limited because drought conditions prevailed throughout Europe.[28,93] In addition, the political and economic situation in the postwar period was precarious.[18] The shortage of forage led to emergency slaughter in 1947: The statistics indicate an increase in the slaughter of horses by 55 percent and of cows by 18 percent. In turn, the emergency slaughter eventually led to shortages of milk and butter, which had to be met with rationing and imports.[18,28,94] Thus, national import volumes for butter in 1947 were almost twice the long-term average and import volumes for condensed milk were even 16 times higher than the average. To alleviate the hardship that had arisen, the federal government granted farmers in the drought areas exceptional aid based on a credit of 40 million francs.[95]

In the extreme years of 2003 and 2018, yield losses in grassland farming were similar or even higher, but shortages of forage were largely compensated for by imports.[96] Border levies were temporarily reduced in 2003 to facilitate imports.[97] Irregularities indicating emergency slaughter are not evident from the statistics for these years.

Timing of drought period is crucial

In arable farming, yields of late crops were markedly affected by drastic drops in 1947. For autumn beets, usually sown between July and

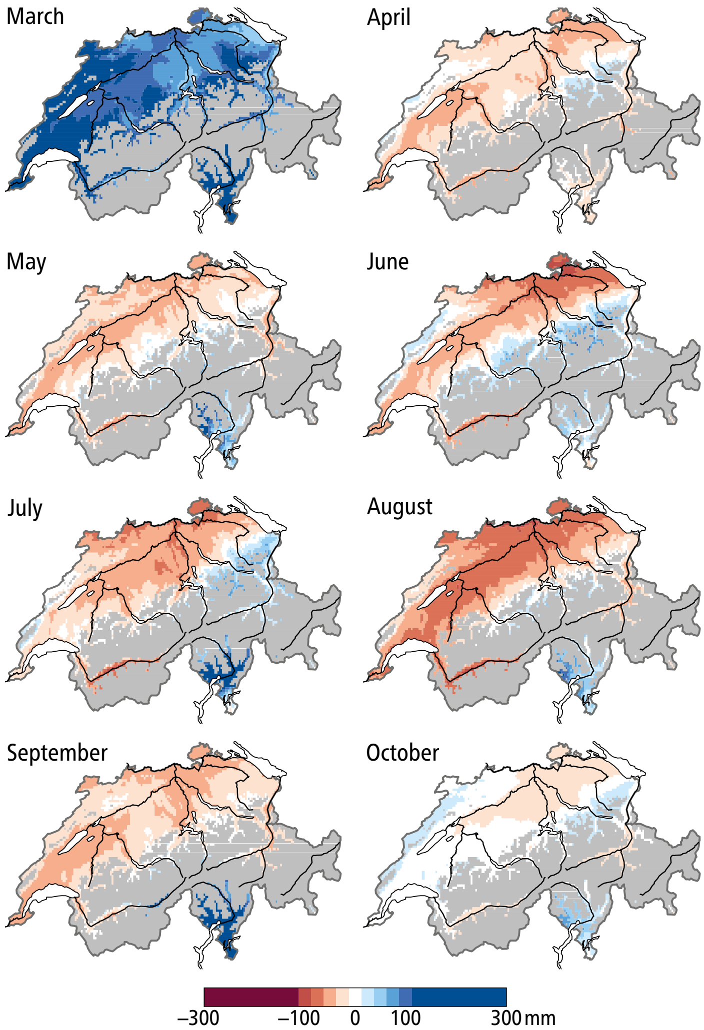

Fig. 6.1: *Temporal and spatial evolution of the drought period in 1947 for areas below 1200 m a.s.l. Shown is the monthly water balance (sum of precipitation minus sum of potential evaporation, in mm). Calculations are based on spatial analyses by the Federal Office of Meteorology and Climatology (MeteoSwiss).[101]*

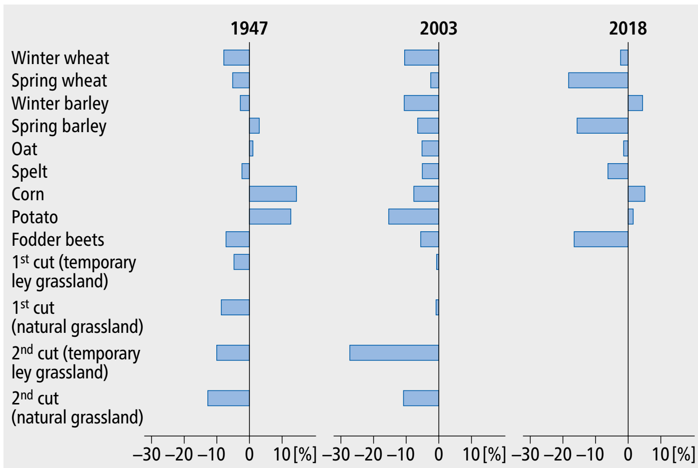

Fig. 6.2: *Yield variances of major crops in the dry years 1947, 2003, and 2018 (1947 compared to 1920–1950 mean[94]; 2003 and 2018 compared to 1990–2020 mean[100]).*

August, mean national yields were 47 percent below the average for the years 1920 to 1950. Similarly, yields of rutabagas, sown in June, were 24 percent below the long-term average.[94] Fodder beet yields were only slightly reduced (–7 percent). This slighter reduction compared to turnips and autumn beets can be explained by the earlier growing season of fodder beets. These were sown around April and could still benefit from abundant rainfall in March 1947. Similar effects of drought on fodder beet yields were also evident in 2003 and 2018 (–5 percent and –16 percent, respectively; Fig. 6.2).

In contrast, the yield of potatoes was 13 percent above the long-term average, the same as national corn yields (14 percent above the long-term average). Given the pronounced climatic anomalies in 1947, these positive yield anomalies are surprising for crops with relatively high water demands. Interestingly, a similar trend is evident for the extreme year of 2018, albeit to a lower extent (+2 – 5 percent yield). This suggests that the timing of the onset of drought is crucial in the context of the cropping cycle, as does the spatial spread of drought and heat. Early crops, such as potatoes or corn, were probably able to benefit from the soil water supply stemming from abundant precipitation in March. A similar effect can be assumed for 2018 when the water deficit between May and June was rather low. In contrast, the drought set in earlier in 2003, and it lasted throughout the entire summer, resulting in substantial yield losses in potato and corn cultivation.

The yield losses in cereal production were comparably low in 1947 (–8 percent for winter wheat). However, the cultivation of cereals was an essential pillar of food supplies for the country's population. Most of the arable land at that time was used for the cultivation of cereals. Hence, a yield loss of 8 percent in the case of winter wheat represented a significant shortfall. In comparison, yield losses for winter wheat in 2003 were slightly higher in percentage terms (–10 percent), but this reduction relates to a much higher yield level. The higher yields in recent decades were achieved through extensive mechanisation of farming practices, improved variety breeding[98], and increased use of mineral fertilizers[94]. Over the period 1990 to 2020, yields of major arable crops were twice to more than three times higher than in the period 1920 to 1950 levels. It is interesting to see that the yields of winter cereals in 2018 were less decimated compared to summer cereals. This can be explained by the fact that the extreme drought in 2018 started later, at a time when winter cereals had already matured but summer cereals were still in the grain filling phase.

Yield losses in a social context

Our comparison of social impacts from yield losses illustrates the large influence of socioeconomic factors on the resilience of the food system to climatic extremes.[93] Yield losses were in a similar range in the three extreme years considered. However, the Swiss population was affected by the extreme weather conditions and their impact on agricultural productivity much more severely in 1947 than in 2003 or 2018. This is due to the developments that led to massive yield increases during the 1950s to the 1970s; even the reduced yields in 2003 were far above the level of the average yields between 1920 and 1950. In addition, the high level of political stability within Europe today also had a stabilising influence on food security.

Potato harvest 1947

Early maturity may have had a substantial influence on the positive yield anomaly for potatoes in 1947, as yields for early varieties in some drought-affected cantons such as Basel, Schaffhausen, and Aargau were slightly higher than yields for late varieties. The overall share of medium-early varieties such as "Bintje" was high in Switzerland at that time.[99] In addition, moisture-favouring fungal diseases such as late blight generally played a major yield-limiting role in potato production during the 1940s, aseffective pesticides were not available at the time. In this respect, the drier conditions in 1947 may have been associated with lower disease pressure and therefore lower yield reductions. As a result of the "cultivation battle" initiated by the Federal Councillor Friedrich Traugott Wahlen in 1940, the area under potato cultivation in 1947 was at almost 70 000 ha. This is much larger than today (11 000 ha in 2020).[99,100] Thus, it is also conceivable that the area under potato cultivation at that time extended to higher, fundamentally cooler locations. In these locations, the above-average temperatures in the summer of 1947 could have had a positive effect on potato yields, while precipitation deficits were less limiting there.

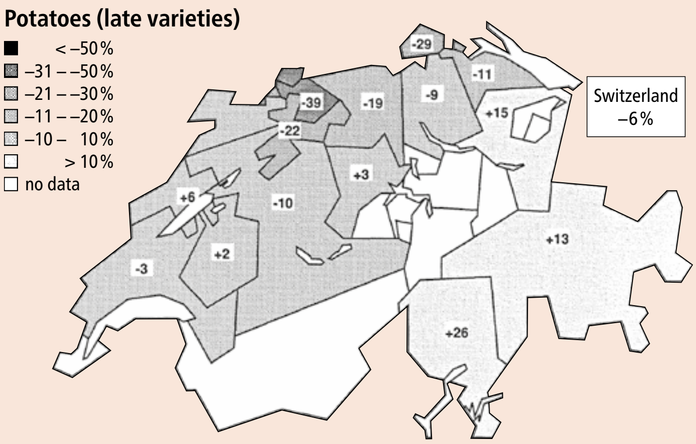

Fig. 6.3: Potato yield in Switzerland 1948 (deviation from the mean of 1944 to 1951 in percentage).[28]

Effects of the 1947 and 2018 droughts on Swiss forests

Summer droughts can lead to significant forest damage. For example, the 2018 summer drought occurred after the severe winter storm "Burglind" and was followed by the warm years of 2019 and 2020. This cascade of extreme events caused massive damage across Switzerland, especially from bark beetle infestations. Here, we show why such damage occurs and how it relates to 1947.

Forest damage of the drought year 1947 was vividly described in reports and articles at that time. However, the damages are difficult to quantify overall, since drought not only leads to immediate damage but also incites medium-term dieback processes. Such dieback processes can affect individual branches of a tree or even entire trees. In contrast, damage from windthrow can be quantified very well because it occurs within a short and well-defined period.[102,103] Nevertheless, there are comparable data on the extent of forest damage as a result of the drought in 1947 versus 2018; this is in terms of bark beetle infestation. Direct damage to forests includes the death of branches, crowns, and entire trees. Indirectly, drought leads to more extensive damage from bark beetle infestations or forest fires, among others. In the following, we take a closer look at the specific forest damages in 1947 and attempt to compare them to the forest damages in the dry year 2018. The year 1947 was considered exceptional for many forests in Switzerland. This can also be seen in the fact that the first forest chronicle was published in the "Schweizerische Zeitschrift für Forstwesen" in the following year[104]. The aim was to record important forest events systematically. Obviously, one was aware of the historical significance of the 1947 drought.

Leaf senescence, death of branches and trees

Various sources report the specific effects that the 1947 drought had on Swiss forests. In very dry locations, leaf senescence, which typically occurs in fall, was observed throughout the country as early as the beginning of August.[104] There are also numerous reports of local forest damage. In the lower areas of the Canton of Basel-Land, the forest was discoloured on the south- and west-facing slopes and on gravel soils as early as the beginning of August. Hornbeams also withered in early August. On the permeable riparian soils of the Birs and Rhine rivers, the crowns of hornbeams, birches, oaks, maples, and willows were largely bare.[105] In the fall of 1947, entire groups of oaks and birches were dead there, while beech trees died less frequently.[106] In Heiligholz, hundreds of spruces withered, and on higher elevations (so-called Tafeljura), young stands of fir and isolated stands of 5 to 10-year-old firs withered widely. Drought damage was also reported from the Rhine area in northern parts of the Cantons of Zurich and Schaffhausen and the Jura slopes on Lake Biel.[106] In the fall of 1947, numerous bare trees, especially sessile oak, beech, and maple, were conspicuous in forest stands. Spruce trees held up better than fir trees. While no major damage was observed in the oak forests on the southern slopes of the Jura Mountains from Biel westward to Saint-Blaise on Lake Neuchâtel, dead oaks and snowball-leaved maples, and more rarely firs, spruces, and beeches, repeatedly stood out. In general, more damage was observed on young trees than on old ones.[106] The drought also led to the death of young spruce stands between Saint-Blaise and Le Landeron, hardwood crops in lower areas of the Canton of Bern, crops in plant nurseries, and planted hardwoods in clearings in the Canton of Zurich.[104] Figure 7.1 shows a map of the reported damage (mainly agriculture) at that time.[107]

Bark beetle infestation of firs and spruces

Bark beetles reproduce under the bark of fir and spruce trees. To do this, they bore holes through the bark. This is difficult in healthy trees because the bark is infused with resin. During prolonged drought, trees produce less resin and are therefore more vulnerable. This can lead to the mass reproduction of bark beetles. Winter storms also affect bark beetle reproduction. They can damage or weaken trees over a wide area, making it easier for bark beetles to bore through dry,

Fig. 7.1: *The areas affected by drought in Switzerland, published on August 27 August 1947, "Schweizer Illustrierte Zeitung".*

damaged bark. After forest damage from winter storms occurred in several Swiss Cantons in 1946,[103] bark beetles multiplied in the warm weather of the following year. Among others, the crooked-toothed fir bark beetle appeared. An initial proliferation spurt of this beetle was observed as early as 1945, which was also a dry year, but seems to have been tied back by the wet conditions of 1946. The bark beetles multiplied even more rapidly in the summer of 1947. Throughout Switzerland, about 340 000 m^3 of beetle wood and 173 000 m^3 of dry wood accrued by 1949 because of the 1947 drought.[108] Since 1800, the bark beetle calamity of 1944–1950 was the largest ever observed.[109]

Forest fires

Increased drought also leads to an increased risk of forest fire. In the summer of 1947, a total of 75 ha of forest burned in two places in the Bedretto Valley (Canton of Ticino), and an unusually high number of fires were reported in the Canton of Valais, but all were quickly extinguished.[104] In the Canton of Graubünden, a large fire destroyed about 170 ha of forest near Tschlin.[110] The forest fires described for the dry year 1947, however, were substantially smaller than the large forest fire on the southern slope of Calanda, which occurred in 1943 (in terms of the area of damaged forests; about 800 ha).[111] They were also smaller than the 300 ha of forest that burned down above Leuk (Canton of Valais) during the heatwave in the summer of 2003.[112] This is arguably because the summer drought of 1947 was less pronounced in the central Alpine valleys than in the central Swiss Plateau and in northern Switzerland (see p. 8).

Comparison of reported forest damages

How does the damage to trees and forests reported for the 1947 drought year compare to the recent 2018 drought year? The records by the various reporters compare well with the damage characteristics of the 2018 summer drought.[8,113,114] All of the symptoms of trees reported for 1947 – from bark cracking to premature leaf discoloration, leaf fall, branch mortality in tree crowns, and death of mature and young trees – were also noted in 2018 and subsequent years (Fig. 7.2). The rapid proliferation of insects, especially bark beetles, as a result of prolonged warmth[115] was also presented correctly for the 1947 case.[116] However, the spatial distribution of the damage from the two events differs. In 1947, the low-lying areas in the Central Plateau, the Jura, and the north of Switzerland suffered the most (Fig. 7.1). In 2018, some areas in Eastern Switzerland (Walensee area from the Linth river

Fig. 7.2: *A forest stand in summer 2020 with partially or completely dead beech trees in Hemishofen SH. The mortality was triggered by the summer drought in 2018. Image: Ulrich Wasem.*

to the Seez valley, the upper Rhine valley) and the low-lying areas of the Valais were additionally affected.[117] In 2018, leaf senescence partly started in mid-July – in 1947 it was early August. In 1947 and the years before, damage from several storms occurred locally in the drought-affected areas (for example, in the Canton of Neuchâtel).[118] In contrast, in 2018, one severe winter storm ("Burglind") swept through the Central Plateau and the Pre-Alps. It resulted in 1.3 million m^3 of windthrow[19] in Switzerland, and it represented the fourth largest storm-damage event since nationwide records began in 1865.[120] As a consequence, the combined effects of this storm, the 2018 summer drought, and the mass reproduction of bark beetles resulted in huge amounts of damaged wood in 2019 and 2020. It was on the order of 1.5 million m^3, significantly exceeding those from 1947.[114] However, it must be considered that timber stocks have increased considerably since World War II.[103,121] Around 1947, forest stands were on average not only less densely stocked (live trees measured in m^3/ha), but also the tree species composition and forest structures did not correspond to today's conditions. In many forests, the proportion of conifer was higher compared to a natural tree species composition and compared to today. This is because conifer had been planted on a large scale in the 19th and 20th centuries.[122] These artificial stands proved to be susceptible to drought, depending on the location. While natural regeneration predominates today, artificial regeneration was widespread in 1947. Accordingly, many plant nurseries and reforestation plots were severely affected by drought. In large parts of the Swiss Central Plateau, the summer drought of 1947 was the most prominent drought year of the 20th century, exceeding even the drought of 2018. However, the summer drought of 1947 affected much smaller areas than that of 2018, which also reached record levels in western Switzerland and the central Alps.

In summary, forest damage was severe in both 1947 and 2018, but the amounts of damaged wood were massively higher in 2018 and subsequent years. The differences in volume can be explained on the one hand by the higher average wood stock per area today, and on the other hand by bark beetle damage, which was promoted by the winter storm Burglind and multiple warm summers. Should the frequency of compound dry spells and winter storms increase in the future, it is to be expected that a drought comparable to 1947 or 2018 could have large impacts on forests on repeated occasions.

Bark beetle control in western Switzerland

The Canton of Neuchâtel reported about 15 000 m^3 of timber that was highly infested by bark beetles in 1948 and another 6000 m^3 in 1949. Mainly fir (about 60 percent) was affected, and spruce to a lesser extent.[123] The situation was even more dire around Lake Biel, where many hectares of drought wood accumulated in fir stands in 1947 already: An area of 40 ha had to be completely cleared, and only 10 to 50 percent of the stocking remained on another area of 60 ha. From 1947 to 1950, about 50 000 m^3 of infested wood accumulated in the Seeland between La Neuveville and Lengnau. As a result, the cutting of timber had to be stopped until 1954, and the price of timber in the region fell by 10 francs per unit due to the oversupply.[116] A few 100 men were employed to combat bark beetle gradation (Fig. 7.3).

Fig. 7.3: *Workers in the Eschenberg forest near Winterthur peeling fir trees infested by the bark beetle and burning the bark in the summer of 1947 (Winterthur Libraries, Winterthur Collection).*

The extreme melting of alpine glaciers in 1947

Hot and dry summers like 1947 have an immediate impact on alpine glaciers. The glacier mass balance as a direct climatic climate signal is correspondingly negative in such weather situations. In the last twenty years, there has been an accumulation of such "glacier-unfavourable" conditions.

Glaciers as sensitive climate indicators

Glaciers are ideal climate indicators, as they clearly reflect past weather patterns. The observed warming in the Alps since the end of the Little Ice Age around 1850 has been accompanied by a considerable melting of all Alpine glaciers.[124] However, glaciers are complex and dynamic systems, as they are influenced by a variety of factors that can only be approximated by close observation. To investigate the relationship between climate and glacier behaviour, two different types of observation can be considered: the glacier mass balance as a direct signal of climate change, and the change in glacier length, which can be perceived visually at the glacier tongue by everyone but is an indirect, delayed, and enhanced climate signal. Both variables are ideally measured every year.

The mass balance describes how much mass a glacier gains or loses over the course of a year. For the mass balance of the glaciers in the Alps, the weather conditions from May to September are particularly decisive. Ablation, i.e., the melting of snow and ice, is stronger the more frequently warm and sunny conditions occur and the longer they last. In addition, precipitation conditions play an important role in the winter season. Increased snowfall leads to greater accumulation, i.e., a stronger increase in glacier mass. This causes new ice to form in higher and thus colder regions of the glacier, the ice is then transported to lower and warmer regions, where ice loss occurs through melting.

The mass balance signal however arrives at the glacier tongue with a certain delay. This is referred to as the response time that a glacier needs until it has found a new state of equilibrium after a climate change – by advancing or retreating. The response time depends to a large extent on the area of the glacier and should not be confused with the reaction time of the glacier tongue to a climatic change. This observable change in glacier length can be two to three times shorter than the response time.[125]

Available glacier mass balance data

Glaciological mass balance data for Central Europe show (Fig. 8.1) that the most negative value of the annual balance since the beginning of measurements was reached in 1946/47. Other years with very negative annual mass balances were 1921, 1950, 2003, 2015, and 2017, and the most negative summer balance was reached in 2003. The years 1947, 1950, 2012, 2015, and 2018 were also characterised by very negative summer balances. For the selected region, the annual balance is primarily determined by the summer balance. The exception is 2018, which has the third most negative summer balance, but a less negative annual balance due to stronger winter precipitation (more positive winter balance). The curves also show that the mean winter balance has changed little, while the summer balances have become significantly more negative over the past forty years. However, in the database of the World Glacier Monitoring Service (WGMS), there are only five glaciers with glaciological mass balance series dating back to 1947. Three of these glaciers are in the Alps (Silvretta, Claridenfirn, Grosser Aletsch). Figure 8.2 shows four of these time series. One of the most detailed mass balance series exists for Storglaciären (Swedish Lapland) since 1945/46. The mass balance for this glacier was also negative in 1947, which corresponds well with elevated temperatures (not shown) and many blocked high-pressure systems (see p. 10). Looking at the individual time series of the three Alpine glaciers, one can see that the year 1947 clearly stands out but does not always represent the absolute most negative value. It should also be noted that these three observational series are based on only a few stake measurements.

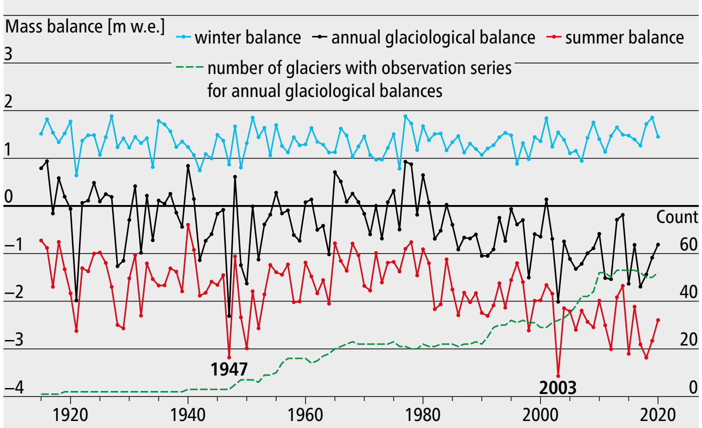

Fig. 8.1: *Annual glaciological mass balances (in metre water equivalent) for the Central European region are shown together with the corresponding number of glaciers with available observations.[124] The most negative annual balance was registered in the hydrological year 1946/47; the most negative summer balance occurred in 2003. Note the low number of observations in the early time.*

Glacier length data

In contrast to the glacier mass balance, measurements of glacier length have been abundant since the 19th century.[126] Moreover, for particularly well-documented glaciers, reconstructions based primarily on historical sources provide information on length changes back to the 16th century.[127] Figure 8.3 shows length changes for selected glaciers in the Western and Central Alps. However, since glacier length change is an indirect, delayed, and integrated climate signal, the effects of individual weather periods (e.g., years with particularly negative mass balance) cannot be determined directly. For certain glaciers, however, increased melting of the glacier tongue can nevertheless be observed in these negative mass balance years, for example at the Rhone glacier.

Consequences of extreme weather situations on glaciers

High air temperature and significantly increased insolation were the effective factors that caused excessive melting of firn and ice in the summer of 1947. Precipitation fell not as snow but as rain, even at high altitudes. Haefeli and Kasser estimated the loss of ice and firn in the entire Swiss Alpine region in the hydrological year 1946/47 at 3.4 billion m^3.[128] M. Huss calculated a maximum ice loss of 5.9 km^3 for the entire Alps in 1947.[129] H. Hoinkes also noted a maximum number of sunshine hours during an ablation period in 1947 (followed by 1950). This period of extreme glacier melt was associated with weak atmospheric circulation; high pressure prevailed for a total of 65 days.[130]

It is also crucial how long the glacier surface remains covered by fresh snow in late spring, as this prevents ablation of the underlying ice. The brighter fresh snow is better able to reflect radiation (higher albedo), and the ice is shielded from the incoming radiation. The opposite situation (compared to 1947) probably occurred several times in the years 1812 to 1817, when snowfall occurred repeatedly at shorter intervals and the ice together with part of the firn remained shielded from solar radiation for a longer time, in extreme cases for an entire summer. As a result, most Alpine glaciers advanced very strongly and rapidly at that time.[131]

Glaciers perform a natural storage function by releasing water, especially during hot droughts, thus providing a supply of water when it is most needed. With the disappearance of glaciers, this important balancing function will be increasingly lost in the near future.[132]

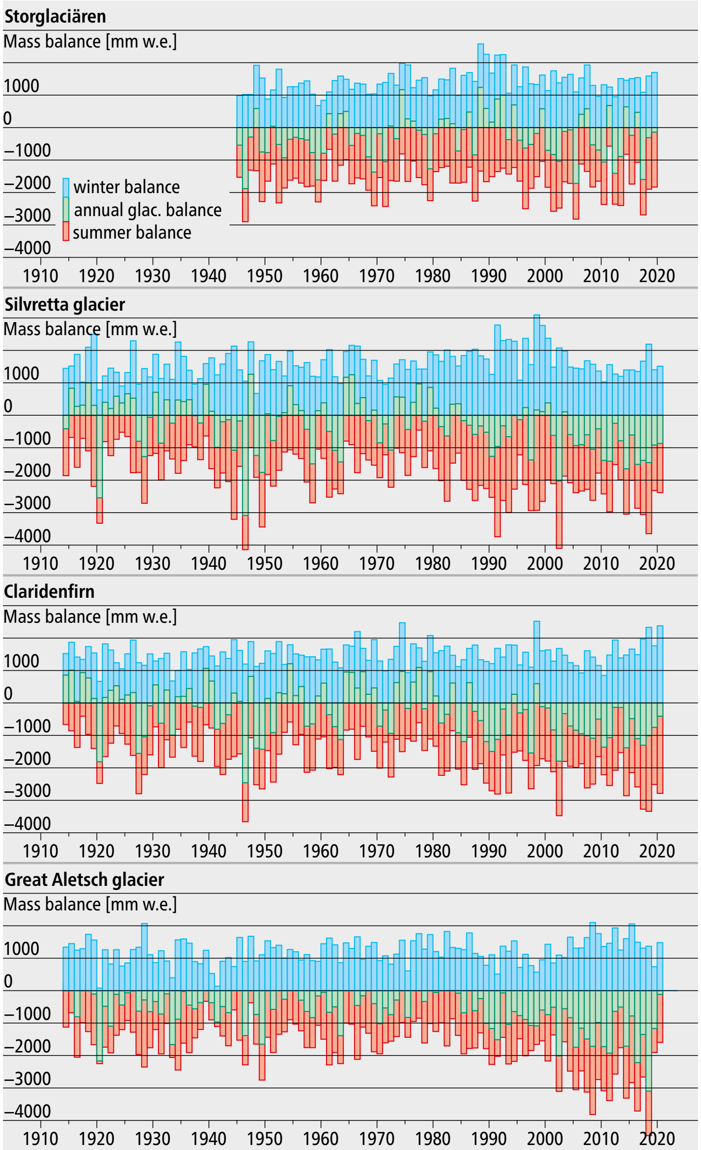

Fig. 8.2: *Glaciological mass balance series for glaciers whose measurement series go back at least to 1947: Storglaciären, Silvretta Glacier, Claridenfirn, Great Aletsch Glacier (data: GLAMOS 1881–2021; WGMS 2021).*

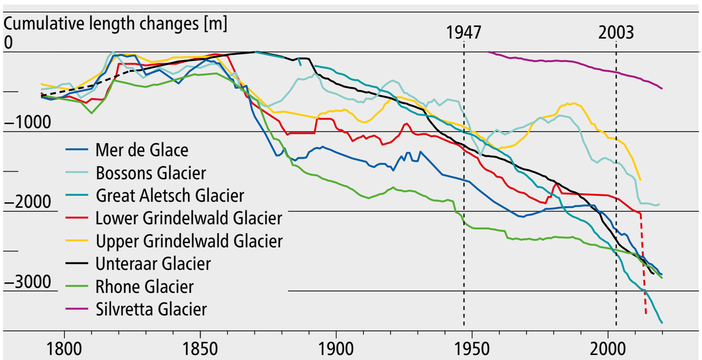

Fig. 8.3: *Length changes of selected glaciers in the Western and Central Alps based on measurements[124,126] or reconstructions (reconstructed values: Nussbaumer, Zumbühl).*

1947, a "catastrophic year" for the glaciers

We get an interesting insight into the effects of the hydrological year 1946/47 from the glacier reports of that time. P.-L. Mercanton writes in "Variations périodiques des glaciers des Alpes suisses"[10] that the hydrological year 1946/47 brought only about three-quarters of the normal precipitation (snow) in winter and the following summer season was much warmer than usual. This led to intense ablation, which not only made the mass accumulation from the previous winter fade but also a good portion of the reserves from previous years. Particularly negative values were measured at the Claridenfirn (2900 m a.s.l.) and Silvretta glacier (3010 m a.s.l.). Discharges in 1947 were also considerable and of exceptional duration. In mid-September, the Rhone at Gletsch had run-off as in mid-summer. According to Mercanton, these exceptional conditions led to a resurgence of interest among glacier observers.

The intense melting of the Rhone glacier (Fig. 8.4) led to disastrous consequences: On the evening of August 9, 1947, an ice dam held back the meltwater; after this ice dam broke, meltwater and ice chunks erupted. Alarmed by the roaring, the people of Belvédère were able to warn the station in Gletsch by telephone to evacuate people. Of the 100 glaciers surveyed in the Swiss Alps in 1947, none were advancing, two were stationary, and 98 were retreating.[10]

In the Eastern Alps, people considered the year a "catastrophic year" for the glaciers. Here, too, the glaciers had almost no accumulation areas left in the summer of 1947. In the Silvretta region, the glaciers became completely snow-free by the beginning of September. The summer of 1947 brought a maximum of surface melting, the firn line moved up to above the upper limit of the accumulation areas and the firn and ice cover of the slopes above the bergschrund melted away in many cases. Many ridges completely lost their snow coverage and were covered with bare ice only, something that even the oldest mountain guides had never experienced.[133]

Fig. 8.4: *The tongue of the Rhone glacier on September 16, 1947, photographed by P.-L. Mercanton.*

Excess mortality during extreme heatwaves in Switzerland

Heat is an important driver of mortality and morbidity in Switzerland: The risk of mortality increases by 16 percent during heat periods in the main Swiss cities,[134] and hospitalizations due to mental disorders increase during heatwaves. However, little is known about the health impacts of historical heat events before 2003, such as the heatwave in 1947. To remedy this, we estimate the excess mortality for eight Swiss cities and assess the health impacts during recent (2003, 2015, 2018) and the historical 1947 heatwaves.

The impact of heat on health has gained public attention since exceptionally warm summers have become more frequent in the last decades. In addition to the record-breaking 2003 European heatwave, four out of the six summers between 2015 and 2021 in Switzerland are considered the warmest summers since the start of the registrations in 1864 (see p. 9). The associated heatwaves events resulted in a substantial death toll, with for example 6.9 percent and 5.4 percent of extra deaths during the two hot summers of 2003 and 2015 in Switzerland, and 2.4 percent in hospital admissions in the latter.[135–137]

The heatwaves affected populations with diverse demographic characteristics and social contexts: What is the role of potential adaptation mechanisms and acclimatisation, changes in demographic exposure and climate? To find some answers, we quantify the all-cause excess mortality during the heatwave of 1947 and compare it to the excess mortality caused by the more recent heatwaves in 2003, 2015, and 2018 in the eight largest Swiss cities (Basel, Bern, Geneva, Lausanne, Lucerne, St. Gallen, Winterthur, and Zurich) in the Swiss Midland, an area that represents a large part of the Swiss population.

Quantify the excess mortality during heatwave periods

Estimation of excess mortality is a well-established approach to assess the health impact of external factors during specific periods such as seasonal infectious diseases (e.g., influenza, COVID-19) or environmental stressors such as heat, or more specifically heatwave events. The term excess mortality refers to the number or percentage of observed deaths beyond the mortality burden we would expect during a specific period according to past trends. This expected mortality is calculated from statistical models based on the seasonal and long-term patterns of past observations.

For our purposes, the all-cause mortality records for the period between 1999 and 2018 are obtained from the Swiss Federal Statistical Office (FSO). Deaths from non-residents and deaths occurring outside of Switzerland are excluded. For the period between 1941 and 1960, we use transcribed historical all-cause mortality records on a weekly level from the "Bulletin des Eidgenössischen Gesundheitsamtes".[138] These do not include stillbirths but apply to both the resident and non-resident population. The quality of these historical vital statistics is assessed to be very good in the literature.[139]

We then calculate the weekly excess mortality as the difference between the observed and the expected mortality for each event (summer period from May to September) and city. The expected number of deaths in each week is estimated using quasi-Poisson regression models, fitted to the observed mortality data in each city and for two different subperiods: 1941–1960 and 1999–2018. This is to avoid any bias from the use of two different data sources. Although the data refers to the same cities, we are unsure whether there were systematic differences in the registration of deaths. Time trends are adjusted for with a linear function of time and a trigonometric polynomial of sine and cosine terms (1-year period), as used in previous assessments.

Results are expressed as excess mortality fraction (percentage) and calculated as excess number of deaths divided by the total number of observed deaths in each week (and multiplied by 100). This relative measure of impact allows a better comparison between the subperiods (1941–1960 and 1999–2018), heatwave episodes, and cities, as it does not reflect differences in the size of the population or length of the study period (i.e., different heatwaves). We summarise the weekly excess mortality as the average across the whole summer period (defined as "Summer excess mortality"), and across the weeks of each heatwave (defined as "Heatwave excess mortality"). We consider a common period of a heatwave for all cities based on the episodes at a national extent. This was the case in the weeks 22 July – 4 August and 12 – 21 August 1947[5], 1 – 13 August 2003[134], 1 – 7 July, and 16 – 24 July 2015[79], 30 July – 8 August 2018[140]. Note that the estimated excess mortality represents an indirect measure of supposed exposure to heat; this is because in the first place, the excess reflects an all-cause deviation from an expected level of mortality. Furthermore, the estimates do not include measures of uncertainty.

Comparison of the excess mortality during the heatwaves

As shown in Table 9.1, the heatwave in the summer of 1947 was particularly harmful for the population in Lucerne and Basel, where excess mortality during the weeks of the heatwave was above 30 percent, followed by Bern and St. Gallen with values of 20 percent or more. The heatwave shock in these areas was also very high. In Lucerne, for instance, excess mortality during the heatwave weeks was approximately six times higher than during the whole summer. This indicates the impact of the 1947 heatwave events. In contrast, we see little or no impact in Lausanne, Geneva, Winterthur, and Zurich (heatwave excess mortality below 10 percent).

	1947		2003		2015		2018	
	HW	Summer	HW	Summer	HW	Summer	HW	Summer
Basel	**32,8**	12,3	**66,0**	13,1	**40,1**	9,3	**40,7**	–0,5
Bern	**23,2**	4,8	**7,4**	1,5	**34,8**	2,5	**31,3**	12,1
Geneva	**5,7**	6,2	**42,1**	11,8	**12,6**	3,9	**13,3**	0,3
Lausanne	**7,0**	–2,1	**25,0**	1,1	**3,0**	–6,1	**10,6**	9,2
Lucerne	**38,5**	6,0	**27,9**	3,0	**25,6**	9,4	**7,9**	3,2
St. Gallen	**19,7**	–4,6	**–7,7**	–2,0	**15,7**	0,3	**8,4**	–3,6
Winterthur	**8,2**	1,8	**21,4**	14,5	**–4,0**	1,0	**1,9**	–9,4
Zurich	**–4,9**	–2,1	**15,8**	8,1	**21,1**	5,1	**42,9**	6,5

Table 9.1: *City-specific excess mortality percentage in summers 1947, 2003, 2015, and 2018. Estimates are reported as the average heatwave excess mortality ("HW") and the average summer excess mortality ("Summer").*

In comparison, the impact of the 2003 heatwave was substantially larger in almost all cities (Fig. 9.1), with excess mortality values of up to 20 percent or more in Lausanne, Lucerne, Winterthur, and Zürich, and of 40 to over 60 percent in Geneva and Basel. The heatwave of 2015 resulted in overall lower excess mortality compared to 2003, and slightly higher compared to 1947. Finally, excess mortality estimates for the 2018 heatwave are similar to the 2015 heatwave in Basel, Bern, and Geneva, and Zurich had a larger death toll.

Overall, the population of the city of Basel was largely affected in all heatwave episodes assessed, while each heatwave impacted differently on the other cities. For example, heatwaves in 1947 affected the city of Lucerne the most, while considerably smaller values are estimated for the more recent heatwaves. The excess mortality during heatwave episodes increased with time in Zurich. Conversely, Geneva was most affected during the 2003 heatwave and much less during the two more recent heatwaves. These diverse spatio-temporal patterns could have been driven by two factors, among others: The first is the complex orography and heterogeneous climate in Switzer-

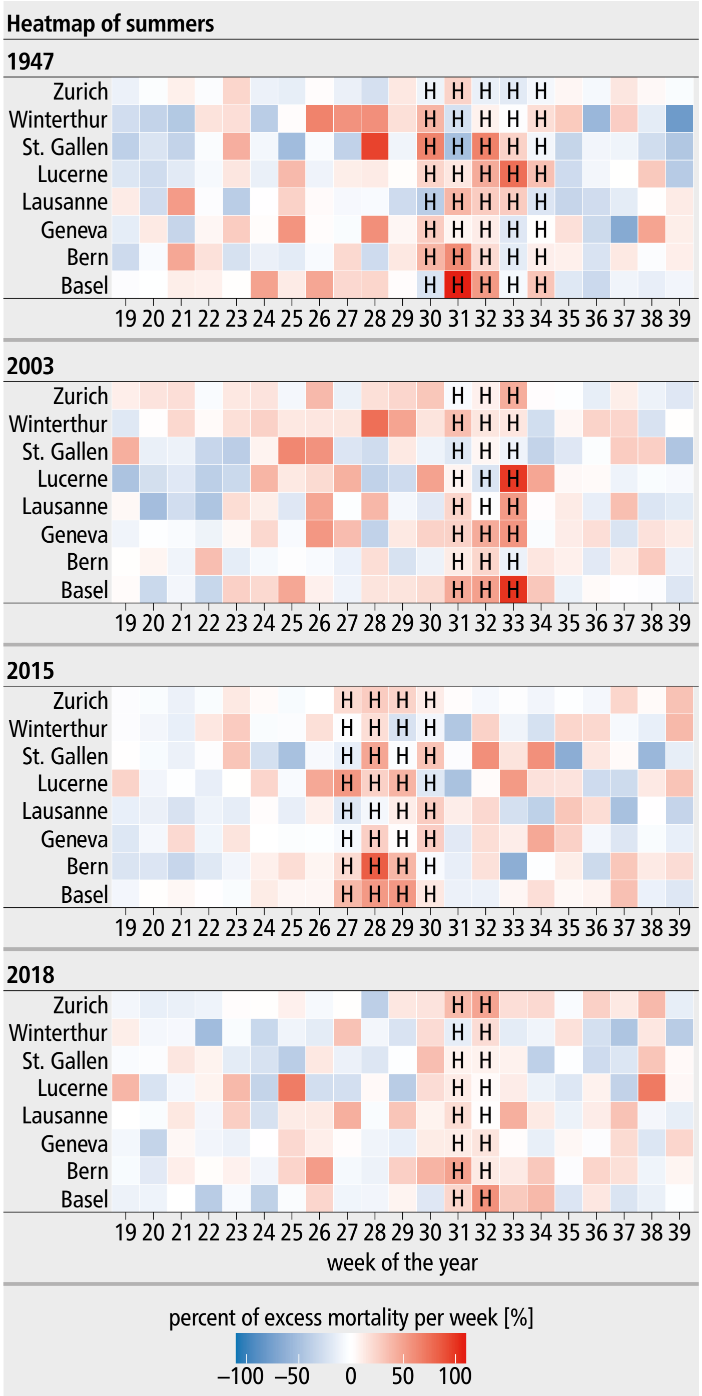

***Fig. 9.1:** Weekly excess mortality (percent) in the cities of Basel, Bern, Geneva, Lausanne, Lucerne, St. Gallen, Winterthur, and Zurich in the summers (May–September) of 1947, 2003, 2015, and 2018. The capital letter "H" indicates the weeks when the heatwave occurred.*

land, which led to differing maximum temperatures and lengths of the heatwave for each location and event – as reported in previous assessments.[79,134,140,141] The second is the diverse characteristics of the population across cities and over time, including demographic structures, socioeconomic and cultural features – which have been previously identified as risk factors for heat-related mortality.[142]

We do not find clear temporal patterns, which would point to a potential adaptation of the population; this contrasts with recent assessments.[138] However, excess mortality during the heatwaves after 2003 was overall slightly lower, despite the accelerated warming over the last decades. This is particularly true for Geneva and Lausanne. A nationwide public health plan was implemented after 2003, and a few Cantons implemented additional measures, including Geneva, Ticino, Vaud, Valais, and Fribourg.[141] This would suggest that the implementation of these additional policies to protect the population from heat (e.g., by introducing warning alerts during heatwave episodes) was efficient in reducing health impacts in the events after 2003.

In addition, we consider that the comparability of the estimates between cities and mainly between the more recent and the 1947 heatwave might be affected by the different demographic structures of the population. According to the Human Mortality Database, 9 percent of the Swiss population were aged 65 or older in 1947, in contrast to 2003, when this proportion had increased to 16 percent. Because old age groups are most vulnerable to heat, and given current trends in ageing, the burden in recent heatwaves could be mostly driven by the high proportion of the old population today compared to the 1940s.

Such burdens could still grow in the future. Today, heat is considered as one of the deadliest environmental hazards with severe impacts on public health and economic activities.[143-145] Climate change is already amplifying these impacts due to the increase in the frequency and severity of heat extremes. It is expected that the impacts on public health will further increase exponentially as warming progresses. This calls for effective adaptation measures,[146,147] which were, of course, not readily available in 1947.

***Fig. 9.2:** People bathing in the Dolder swimming pool, Comet. Photo AG, Zurich, 1947.*

Summer heat and drought: an excursion into Switzerland's climate future

Climate scenarios on a global and regional scale show that the warming already observed will continue in the future. Its extent will be determined by future anthropogenic green house gas emissions. Even if the 2-degree target of the Paris agreement on climate protection was reached, temperatures in Switzerland will continue to rise at least until the middle of the century. Conditions as in the summer of 1947 are thus about to become more and more likely and, under certain circumstances, will become the norm. Based on a fictitious future extreme summer, we show what conditions we will have to expect in Switzerland in the future if efforts to reduce greenhouse gas emissions worldwide will not be successful.

Global and european climate scenarios

The summer of 1947 was an extreme event at the time of its occurrence, but it is already far less exceptional today due to ongoing climate change and the warming observed to date (see p. 9). Since pre-industrial times, mean temperatures in Switzerland have risen by around 2 °C,[17] and recent decades have seen an increased occurrence of summer droughts.[26] There is widespread agreement that these climatic changes do not represent natural variability, but are caused by human activities and the continued emission of greenhouse gases.[148] This human influence will also continue to affect our climate in the future.

The decisive factors for the extent of climate change by the end of the 21st century are the total amount of greenhouse gases emitted in the future as well as the effectiveness of natural and engineered sinks that can remove some of the emitted greenhouse gases from the atmosphere. Significant and rapid reductions in human emissions could limit the increase in global mean temperature to 2 °C and possibly even to 1.5 °C compared to pre-industrial times. This is the goal set by the international community in the Paris Climate Agreement of 2015. However, the climate protection measures currently announced by individual countries (as of January 2022) will probably not be sufficient to achieve this goal.[149]

Global climate models are used to estimate the influence of human greenhouse gas emissions on the global climate. These are complex mathematical-physical representations of the climate system and include all key climate processes in the atmosphere, ocean, and at the land surface. The models use prescribed specific future pathways of human greenhouse gas emissions, based on which they simulate climatic changes. Since the results depend on the chosen emission pathway on time scales of several decades, they are referred to as climate scenarios or climate projections – this is in contrast to weather and climate forecasts with their shorter prediction periods. However, due to the enormous computing power required by global climate models, their spatial resolution of 100 to 150 km is usually too coarse to represent regional features of the climate. This is especially true for complex terrain such as the Alpine region. Therefore, regional climate models are often used, which do not cover the entire globe but only a specific region and can thus be operated with a higher spatial resolution of a few kilometres.[150] At their boundaries, these models obtain their information on the large-scale atmospheric state from global climate simulations.

Figure 10.1 shows the projected summer temperature and precipitation change over Europe until the end of the century assuming a business-as-usual scenario without global climate protection efforts (Representative Concentration Pathway RCP8.5). The analysis is based on a large number of regional climate simulations of the EURO-CORDEX initiative.[151,152] Over almost all of Europe, a further increase in summer temperature of more than 3 °C compared to the 1981 – 2010 reference period is expected (Fig. 10.1a). An even stronger warming of 5 °C or more is expected over southern Europe. This strong warming in the southern part of Europe encompasses also the Alpine region and Switzerland. The reasons for this so-called Mediterranean amplification are not fully understood but are probably linked to changes in the vertical profile of atmospheric temperature.[153,154] This amplification is also at least partly responsible for the marked summer drying signal expected for central and southern Europe (Fig. 10.1b). The Alpine region and Switzerland are also affected by a decrease of summer precipitation, while a slight increase in summer precipitation is expected for large parts of northern Europe.

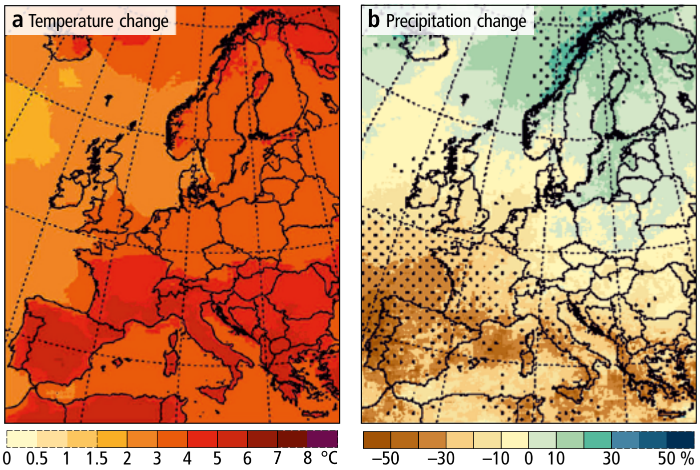

Fig. 10.1: *a) Expected change of summer temperature and b) summer precipitation (June–August) over Europe until the end of the century compared to the reference period 1981 – 2010 for a scenario without climate protection (RCP8.5). Shown is the median of the EURO-CORDEX model ensemble.[151,152] Dotted areas in the right figure indicate grid cells where 90 percent or more of all models agree on the direction of precipitation change.[2]*

Climate scenarios for Switzerland

What do these regional climate projections look like for Switzerland? This question is answered in detail in the current "CH2018 Climate Scenarios for Switzerland".[2,155] They are the official reference scenarios and an important basis for the Swiss adaptation strategy.[156] The scenarios were developed by a research consortium led by MeteoSwiss and ETH Zurich and under the umbrella of the National Centre for Climate Services (NCCS). To further increase the spatial detail of the EURO-CORDEX scenarios and correct for systematic model errors, a statistical downscaling and error correction procedure was applied, and the model projections were downscaled to a high-resolution 2-kilometre grid for Switzerland and to individual station locations.[157]

Consistent with the European projections, we expect further summer warming (Fig. 10.2a). Depending on the emissions scenario, this warming will amount to about 5 °C (scenario without climate protection, RCP8.5) or about 1.3 °C (scenario with climate protection, RCP2.6) by the end of the 21st century, with some considerable model uncertainty around these central estimates. In the optimistic emission scenario RCP2.6, which would most likely be ensured with the achievement of the Paris 2-degree target, it appears that further warming would in principle only occur until mid-century, and mean summer temperatures would subsequently remain at a relatively stable level. The projected development of summer precipitation amounts is somewhat less clear (Fig. 10.2b). In the climate protection scenario (RCP2.6), only slight decreases are expected by the end of the century (about –4 percent). However, if greenhouse gas emissions remain unabated (RCP8.5), a significant decrease of summer precipitation is projected for the mid-century and beyond (about –21 percent). The probability of occurrence of a hot and dry summer similar to 1947 is therefore likely to increase significantly in the future and become the norm, at least in a scenario without climate protection.

The mean changes described will have an impact on many downstream systems and indicators. As an example, Figure 10.4 shows the spatial distribution of the number of hot days in the observations of the reference period 1981–2010 as well as towards the end of the century for a scenario with and without climate protection. A hot day is defined as a day with a maximum temperature above 30 °C and is usually associated with a noticeable heat load for the human body. In the climate of the reference period, hot days occur in the Swiss Plateau, in the Geneva region, in Ticino, and in warm valleys on average no more than 15 times per year (Fig. 10.4a). By the end of the century, the frequency of occurrence will increase significantly in both scenarios and will also include regions that have not yet been affected. In a scenario with climate protection (Fig. 10.4b), more than twenty hot days are expected in the southern regions and warm valleys, and the phenomenon of hot days will extend into the area of the northern foothills of the Alps. Even stronger changes are expected for a scenario without climate protection (Fig. 10.4c): Here, more than thirty hot days per year and in some cases even up to sixty hot days per year are to be expected in large parts of Switzerland towards the end of the century. A strong heat load will also become apparent in the northern Alpine region or the tributary valleys.

An extreme summer of the future

What might an extremely hot and dry summer, like the summer of 1947, look like in the future? And what would its consequences be? A master thesis (ETH Zurich and MeteoSwiss)[158] addressed these questions based on the "CH2018 climate scenarios for Switzerland". For this purpose, a future, fictitious "summer 2090" was identified, which was defined to be similarly extreme with respect to the summer mean temperature expected towards the end of the century over Switzerland as the summers 1947 or 2003 were in their respective prevailing summer climates. A scenario without climate protection (RCP8.5) was assumed. This future summer thus was simulated by one

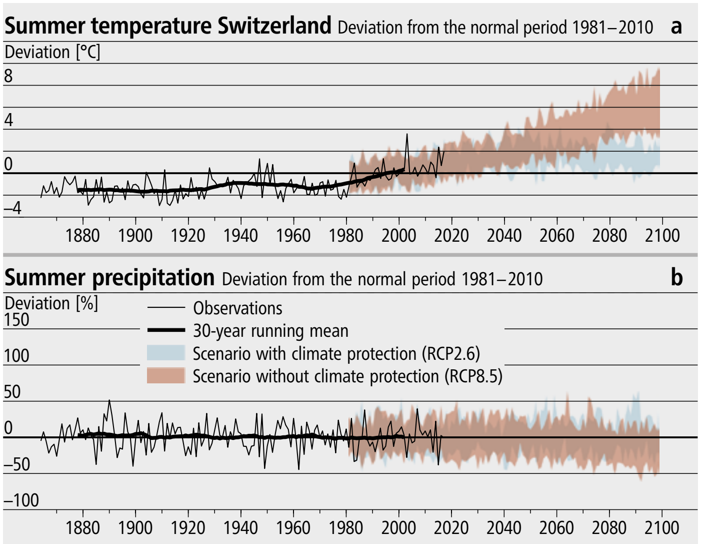

Fig. 10.2: *Previously observed and projected future development of summer mean temperature (top) and summer precipitation (bottom; June–August in each case) over the area of Switzerland. The coloured areas show the model uncertainty range for a scenario with climate protection (RCP2.6, blue) and a scenario without climate protection (RCP8.5, red).*[2]

The summer of 1947 in a climate of the future

The summer of 1947 was considered exceptionally warm at that time. Since then, however, the climate has warmed considerably, and it will continue to warm in the coming decades. How normal will a summer like 1947 become in a future climate? To answer this question, we compare the mean temperature of the summer half-years 1947, 2003, and 2018 with the expected climate at the end of the 21st century. We determine the Swiss mean temperature for the CH2018-scenarios as a weighted average of 19 stations.[20] We approximate the distribution of projected summer half-year temperatures with a normal distribution for each climate model simulation. Because the trend in the data has not been removed, the year-to-year variability may be somewhat too high, that is, the range of the distribution may be somewhat too large. We calculate the mean future temperature of a summer half-year over the thirty years 2070–2099 and for both projections.

Figure 10.3 shows that a summer half-year will be warmer than 11 °C towards the end of the century in most cases, regardless of the assumed emissions scenario. The expected Swiss mean temperature for the summer half-year and all climate model simulations is 11.8 °C with RCP2.6 and 15.2 °C with RCP8.5. Thus, summer half-years warmer than 1947 will be very common at the end of the century, even under a scenario with climate protection. Without climate protection, significantly warmer summers than 1947, 2003, and 2018 are to be expected: A summer like 1947 would then even be exceptionally cold and would only occur very rarely. If, on the other hand, climate protection measures are partially implemented (RCP4.5), the summers of 2003 and 2018 would then roughly correspond to an average future summer.

In a period of merely 150 years, the significance of the summer of 1947 is about to change fundamentally. If it was still an exceptionally warm event at that time, it is expected that the summer temperature observed in 1947 will often be exceeded by the end of the 21st century. Without climate protection measures taken, 1947 would even become an exceptionally cool summer in a future climate.

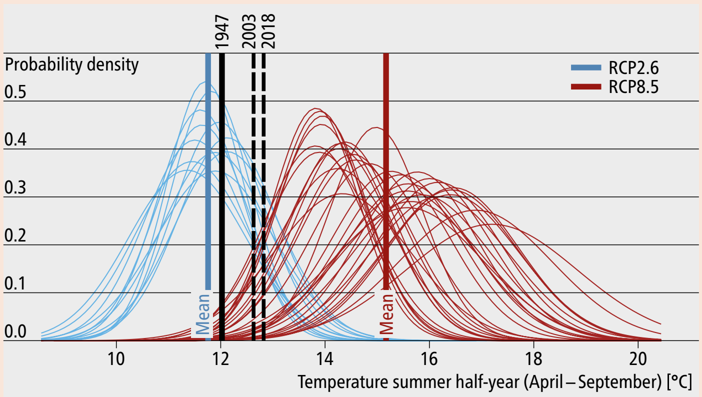

Fig. 10.3: *Distribution of summer half-year (April–September) temperature for the late century period (2070–2099). A normal distribution was fitted for each climate model simulation (thin coloured lines). The trend in the data was not removed. The coloured vertical lines show the mean over all summer half-year temperatures of the respective RCP. Also shown are the observed temperatures for the summer half-years of 1947 (12.0 °C), 2003 (12.6 °C), and 2018 (12.8 °C). For all data, the Swiss average temperature was determined.*[20]

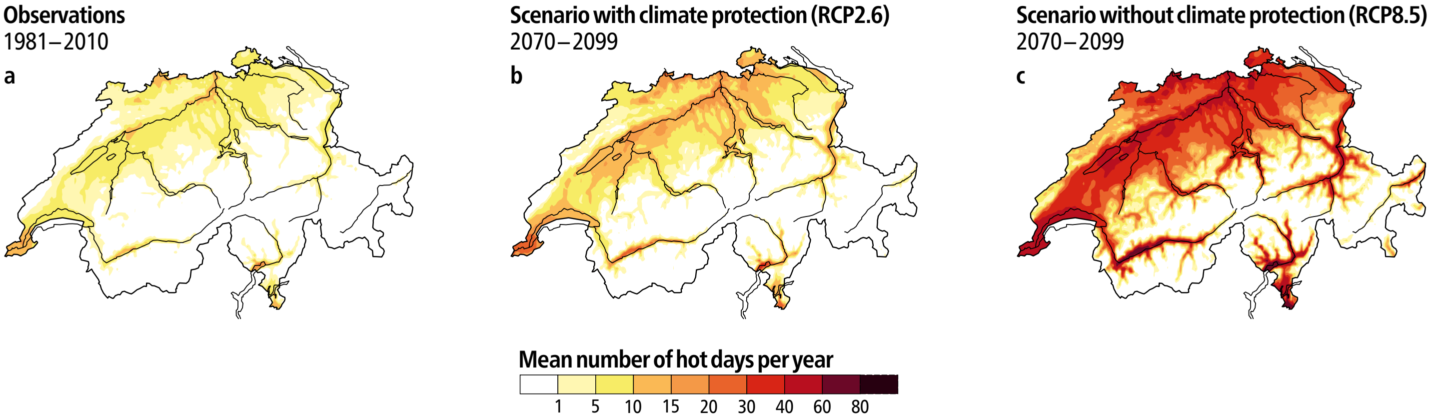

Fig. 10.4: *Spatial distribution of the mean number of hot days (days with maximum temperature >30 °C) per year in a) observations of the reference period 1981–2010 and towards the end of the century, in b) a scenario with climate protection (RCP2.6), and in c) a scenario without climate protection (RCP8.5).*[2]

of the underlying EURO-CORDEX model chains, statistically error-corrected, and downscaled to a finer spatial resolution within CH2018.

It is shown that the future extreme "summer 2090" will significantly exceed the temperature and precipitation conditions of the year 1947 (Fig. 10.5). Summer mean temperatures above 20 °C will prevail over larger parts of Switzerland. Even in high-altitude regions of the Alps, the mean temperature rarely drops below 10 °C, and parts of the Swiss Plateau and western Switzerland show values above 25 °C (Fig. 10.5b). Over the whole of Switzerland, the "summer 2090" will more than 5 °C warmer than the summer of 1947, and differences of even more than 7 °C are found for some parts (Fig. 10.5c). Also, the summer drought will be again much more pronounced in 2090 than in 1947. Almost all of Switzerland shows mean monthly precipitation amounts of less than 100 mm (Fig. 10.5, bottom row). Compared to the summer of 1947, which was already very dry at that time, this means a further reduction of precipitation amounts by more than 40 percent in most regions, in southern and western Switzerland even by more than 60 percent in some cases (Fig. 10.5).

This example illustrates the extreme conditions to which Switzerland's summer climate is heading without global climate protection efforts and gives an idea of the necessary efforts in climate adaptation. Even if water bodies may still provide short-term cooling during future summer heatwaves (Fig. 10.6), planning long-term measures to deal with the changes is pressing. Climate protection and climate adaptation are of outstanding importance also for a country with a comparatively moderate climate like Switzerland.

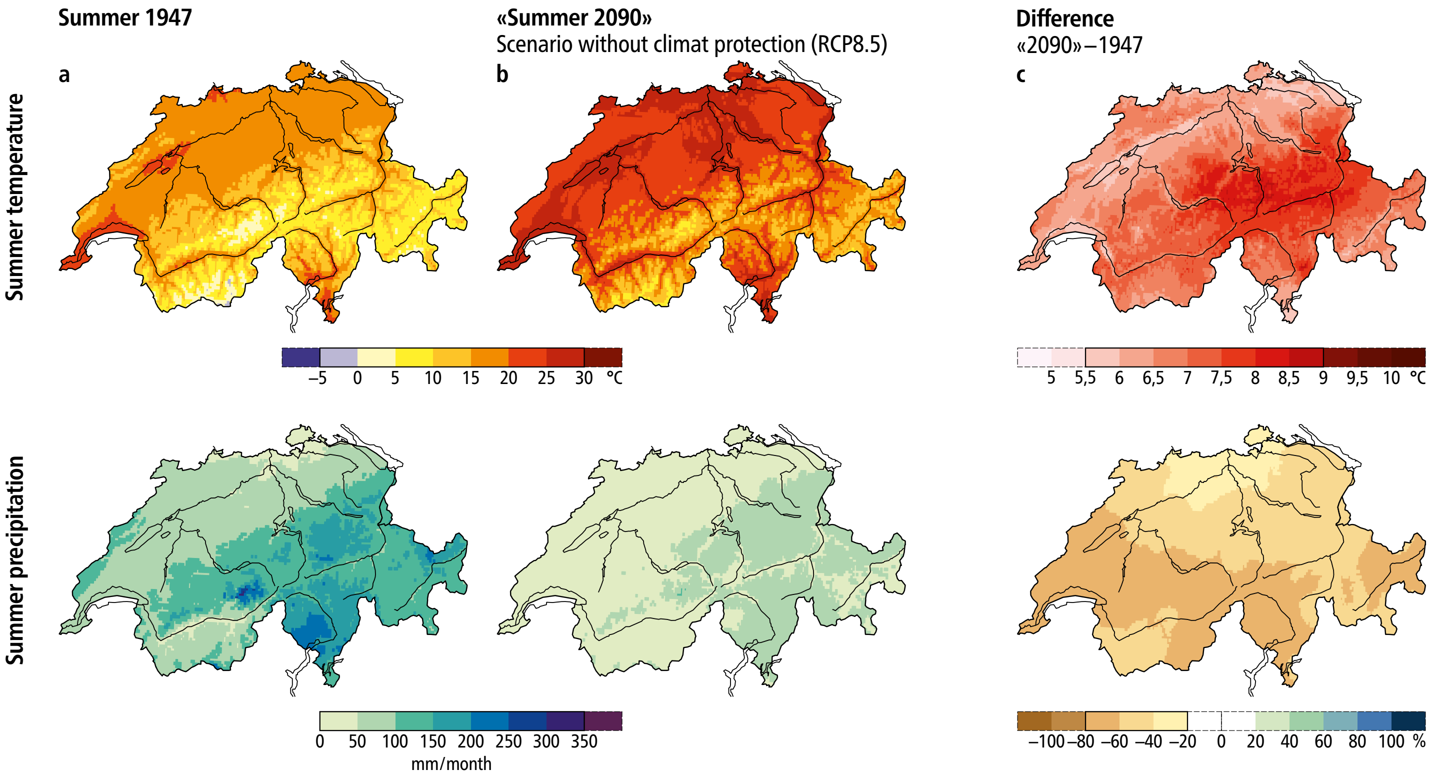

Fig. 10.5: *Spatial distribution of summer mean temperature (top) and summer precipitation (bottom; June–August in each case) a) for the year 1947 as well as b) for a future extreme summer "2090" in a scenario without climate protection (RCP8.5) and c) difference "summer 2090" minus summer 1947.*[158]

Fig. 10.6: *The Rhine in Basel will continue to provide cooling during the even hotter summer months (© Shutterstock).*

References

1 BAFU (Hrsg.). Hitze und Trockenheit im Sommer 2018. Auswirkungen auf Mensch und Umwelt. *Bundesamt für Umwelt, Bern. Umwelt-Zustand* **Nr. 1909**, 96 (2019).

2 CH2018. *CH2018 – Climate Scenarios for Switzerland, Technical Report. National Centre for Climate Services,* Zurich (2018).

3 Vogel, M. M., Zscheischler, J., Wartenburger, R., Dee, D. & Seneviratne, S. I. Concurrent 2018 Hot Extremes Across Northern Hemisphere Due to Human-Induced Climate Change. *Earth's Future* **7**, 692–703 (2019).

4 BAFU (Hrsg.). Hitze und Trockenheit im Sommer 2015. Auswirkungen auf Mensch und Umwelt. *Bundesamt für Umwelt, Bern. Umwelt-Zustand* **Nr. 1629** 108 (2016).

5 Grütter, J., Lehmann, S., Auchmann, R., Martius, O. & Brönnimann, S. The heatwaves in Switzerland in summer 1947. *Geogr. Bernensia* **G89** 69–80 (2013).

6 Hirschi, E., Auchmann, R., Martius, O. & Brönnimann, S. The 1945–1949 droughts in Switzerland. *Geogr. Bernensia* **G89**, 81–90 (2013).

7 Calanca, P. Climate change and drought occurrence in the Alpine region: How severe are becoming the extremes? *Glob. Planet. Change* **57**, 151–160 (2007).

8 Rathgeb, U., Bürgi, M. & Wohlgemuth, T. Waldschäden wegen Dürre von 1864 bis 2018 in der Schweiz und insbesondere im Kanton Zürich. *Schweizerische Zeitschrift für Forstwesen* **171**, 249–256 (2020).

9 Baumgartner, A. Niederschlagsschwankungen und Dürregefährdung mit Bezug auf den Waldbau. *Forstwissenschaftliches Cent.* **69**, 636–662 (1950).

10 Mercanton, P.-L. Les variations périodiques des glaciers des Alpes suisses. Soixante-huitième rapport – 1947. *Les Alpes* **24**, 8 (1948).

11 Dewitz, H. A. Versteppung bedroht unseren Kontinent. *Die Zeit* **Nr. 33** (1947).

12 Schweizer Filmwochenschau. Available at: *https://memobase.ch/de/recordSet/bar-001*.

13 Research on this issue was supported by the Swiss National Science Foundation (WeaR project, 188701) and the European Commission (ERC Grant PALAEO-RA, 787574).

14 Matthias Röthlisberger's contribution was funded by the European Research Council (ERC) under the Horizon 2020 program, through grant number 787652.

15 Kaspar Staub would like to thank the Foundation for Scientific Research at the University of Zurich (STWF-21-011) for funding and Inga Birkhäuser and Julia Simola for their help in transcribing the historical data.

16 MeteoSchweiz. MeteoSchweiz Blog vom 18. Januar 2021. (2021). Available at: *https://www.meteoschweiz.admin.ch/home/aktuell/meteoschweiz-blog/meteoschweiz-blog.subpage.html/de/data/blogs/2021/1/waermstes-jahrzehnt-sein-messbeginn.html*.

17 BAFU (Hrsg.). Klimawandel in der Schweiz. Indikatoren zu Ursachen, Auswirkungen, Massnahmen. *Bundesamt für Umwelt, Bern. Umwelt-Zustand* **Nr. 2013**, 105 (2020).

18 Mörikofer, W. Die Trockenheit des Sommers 1947 in der Schweiz. *Prisma* **2 (7)**, 201–206 (1947).

19 MZA. Die Dürre des Sommers 1947. in *Annalen der Schweizerischen Meteorologischen Zentralanstalt 1947, 84. Jahrgang Zürich* (1948).

20 Begert, M. & Frei, C. Long-term area-mean temperature series for Switzerland – Combining homogenized station data and high resolution grid data. *Int. J. Climatol.* **38**, 2792–2807 (2018).

21 Bider, M. Die ungewöhnliche Wärmeperiode 1947 statistisch untersucht. *Experientia* **IV/4**, 14 (1948).

22 MeteoSchweiz. Hitze und Trockenheit im Sommerhalbjahr 2018 – eine klimatologische Übersicht. *Fachbericht MeteoSchweiz* **272**, 38 (2018).

23 Bader, S. Die extreme Sommerhitze im aussergewöhnlicher Witterungsjahr 2003. *Arbeitsbericht der MeteoSchweiz* **200**, 23 (2004).

24 BUWAL. Auswirkungen des Hitzesommers 2003 auf die Gewässer. *Schriftenreihe Umwelt Nr. 369* 174 (2004).

25 Pfister, C. & Rutishauser, M. Dürresommer im Schweizer Mittelland seit 1525. *Unterlagen zum OcCC/ProClim- Work.* **1525**, (2000).

26 Scherrer, S. C., Hirschi, M., Spirig, C., Maurer, F. & Kotlarski, S. Trends and drivers of recent summer drying in Trends and drivers of recent summer drying in Switzerland. *Env. Res. Commun.*, 4 (2022).

27 MZA. Description synoptique de l'évolution du temps au cours des mois particulièrement secs de l'année 1947. in: *Annalen der Schweizerischen Meteorologischen Zentralanstalt 1947, 84. Jahrgang, Zürich* (1948).

28 Schorer, M. Extreme Trockensommer in der Schweiz und ihre Folgen für Natur und Wirtschaft. *Geographica Bernensia* **G40**, Bern (1992).

29 Isotta, F. A., Begert, M. & Frei, C. Long-Term Consistent Monthly Temperature and Precipitation Grid Data Sets for Switzerland Over the Past 150 Years. *J. Geophys. Res. Atmos.* **124**, 3783–3799 (2019).

30 Bieli, M., Pfahl, S. & Wernli, H. A lagrangian investigation of hot and cold temperature extremes in Europe. *Q. J. R. Meteorol. Soc.* **141**, 98–108 (2015).

31 Zschenderlein, P., Fink, A. H., Pfahl, S. & Wernli, H. Processes determining heat waves across different European climates. *Q. J. R. Meteorol. Soc.* **145**, 2973–2989 (2019).

32 Pfahl, S. & Wernli, H. Quantifying the relevance of atmospheric blocking for co-located temperature extremes in the Northern Hemisphere on (sub-)daily time scales. *Geophys. Res. Lett.* **39**, (2012).

33 Sousa, P. M., Trigo, R. M., Barriopedro, D., Soares, P. M. M. & Santos, J. A. European temperature responses to blocking and ridge regional patterns. *Clim. Dyn.* **50**, 457–477 (2018).

34 Röthlisberger, M. & Martius, O. Quantifying the Local Effect of Northern Hemisphere Atmospheric Blocks on the Persistence of Summer Hot and Dry Spells. *Geophys. Res. Lett.* **46**, 10101–10111 (2019).

35 Altenhoff, A. M., Martius, O., Croci-maspoli, M., Schwierz, C. & Davies, H. C. Linkage of atmospheric blocks and synoptic-scale Rossby waves: A climatological analysis. *Tellus, Ser. A Dyn. Meteorol. Oceanogr.* **60**, 1053–1063 (2008).

36 Woollings, T. *et al.* Blocking and its Response to Climate Change. *Curr. Clim. Chang. reports* **4**, 287–300 (2018).

37 Fink, A. H. *et al.* The 2003 European summer heatwaves and drought--synoptic diagnosis and impacts. *Weather* **59**, 209–216 (2004).

38 Black, E., Blackburn, M., Harrison, G., Hoskins, B. & Methven, J. Factors contributing to the summer 2003 European heatwave. *Weather* **59**, 217–223 (2004).

39 Spensberger, C. *et al.* Dynamics of concurrent and sequential Central European and Scandinavian heatwaves. *Q. J. R. Meteorol. Soc.* **146**, 2998–3013 (2020).

40 Schneidereit, A. *et al.* Large-Scale Flow and the Long-Lasting Blocking High over Russia: Summer 2010. *Mon. Weather Rev.* **140**, 2967–2981 (2012).

41 Trenberth, K. E. & Fasullo, J. T. Climate extremes and climate change: The Russian heat wave and other climate extremes of 2010. *J. Geophys. Res. Atmos.* **117**, 17103 (2012).

42 Fragkoulidis, G., Wirth, V., Bossmann, P. & Fink, A. H. Linking Northern Hemisphere temperature extremes to Rossby wave packets. *Q. J. R. Meteorol. Soc.* **144**, 553–566 (2018).

43 Shutts, G. J. The propagation of eddies in diffluent jetstreams: Eddy vorticity forcing of 'blocking' flow fields. *Q. J. R. Meteorol. Soc.* **109**, 737–761 (1983).

44 Steinfeld, D. & Pfahl, S. The role of latent heating in atmospheric blocking dynamics: a global climatology. *Clim. Dyn.* **53**, 6159–6180 (2019).

45 Röthlisberger, M., Frossard, L., Bosart, L. F., Keyser, D. & Martius, O. Recurrent Synoptic-Scale Rossby Wave Patterns and Their Effect on the Persistence of Cold and Hot Spells. *J. Clim.* **32**, 3207–3226 (2019).

46 Hersbach, H. *et al.* The ERA5 global reanalysis. *Q. J. R. Meteorol. Soc.* **146**, 1999–2049 (2020).

47 Sprenger, M. & Wernli, H. The LAGRANTO Lagrangian analysis tool – Version 2.0. *Geosci. Model Dev.* **8**, 2569–2586 (2015).

48 Scherrer, S. C., Croci-Maspoli, M., Schwierz, C. & Appenzeller, C. Two-dimensional indices of atmospheric blocking and their statistical relationship with winter climate patterns in the Euro-Atlantic region. *Int. J. Climatol.* **26**, 233–249 (2006).

49 Slivinski, L. C. *et al.* Towards a more reliable historical reanalysis: Improvements for version 3 of the Twentieth Century Reanalysis system. *Q. J. R. Meteorol. Soc.* **145**, 2876–2908 (2019).

50 Hoskins, B. J. & Karoly, D. J. The Steady Linear Response of a Spherical Atmosphere to Thermal and Orographic Forcing . *J. Atmos. Sci.* **38**, 1179–1196 (1981).

51 Walter, K., Luksch, U. & Fraedrich, K. A Response Climatology of Idealized Midlatitude Thermal Forcing Experiments with and without a Storm Track. *J. Clim. Clim.* **14**, 467–484 (2001).

52 Cassou, C., Terray, L. & Phillips, A. S. Tropical Atlantic Influence on European Heat Waves. *J. Clim.* **18**, 2805–2811 (2005).

53 Duchez, A. *et al.* Drivers of exceptionally cold North Atlantic Ocean temperatures and their link to the 2015 European heat wave. *Environ. Res. Lett.* **11**, 074004 (2016).

54 Ghosh, R., Müller, W. A., Baehr, J. & Bader, J. Impact of observed North Atlantic multidecadal variations to European summer climate: a linear baroclinic response to surface heating. *Clim. Dyn.* **48**, 3547–3563 (2017).

55 Zhang, R., Sun, C., Zhu, J., Zhang, R. & Li, W. Increased European heat waves in recent decades in response to shrinking Arctic sea ice and Eurasian snow cover. *npj Clim. Atmos. Sci. 2020 31* **3**, 1–9 (2020).

56 Petoukhov, V., Rahmstorf, S., Petri, S. & Schellnhuber, H. J. Quasiresonant amplification of planetary waves and recent Northern Hemisphere weather extremes. *Proc. Natl. Acad. Sci. U. S. A.* **110**, 5336–5341 (2013).

57 Kornhuber, K., Petoukhov, V., Petri, S., Rahmstorf, S. & Coumou, D. Evidence for wave resonance as a key mechanism for generating high-amplitude quasi-stationary waves in boreal summer. *Clim. Dyn.* **49**, 1961–1979 (2017).

58 Wirth, V. Waveguidability of idealized midlatitude jets and the limitations of ray tracing theory. *Weather Clim. Dyn.* **1**, 111–125 (2020).

59 Trenberth, K. E. & Shea, D. J. Atlantic hurricanes and natural variability in 2005. *Geophys. Res. Lett.* **33**, 12704 (2006).

60 Hadley Centre for Climate Prediction and Research. HadISST1.1 – Global Monthly Mean Gridded SSTs (1870–2015). *NCAS Br. Atmos. Data Cent.* (2007).

61 Mitchell, D. *et al.* Attributing human mortality during extreme heat waves to anthropogenic climate change. *Environ. Res. Lett.* **11**, 074006 (2016).

62 Bastos, A. *et al.* Impacts of extreme summers on European ecosystems: a comparative analysis of 2003, 2010 and 2018. *Philos. Trans. R. Soc. B* **375**, 20190507 (2020).

63 Beillouin, D., Schauberger, B., Bastos, A., Ciais, P. & Makowski, D. Impact of extreme weather conditions on European crop production in 2018. *Philos. Trans. R. Soc. B* **375**, (2020).

64 Meehl, G. A. & Tebaldi, C. More intense, more frequent, and longer lasting heat waves in the 21st century. *Science* **305**, 994–997 (2004).

65 Cattiaux, J. *et al.* Winter 2010 in Europe: A cold extreme in a warming climate. *Geophys. Res. Lett.* **37**, L20704 (2010).

66 Fischer, E. M., Seneviratne, S. I., Lüthi, D. & Schär, C. Contribution of land-atmosphere coupling to recent European summer heat waves. *Geophys. Res. Lett.* **34**, 1–6 (2007).

67 Seneviratne, S. I., Lüthi, D., Litschi, M. & Schär, C. Land-atmosphere coupling and climate change in Europe. *Nature* **443**, 205–209 (2006).

68 Koster, R. D. et al. Regions of Strong Coupling Between Soil Moisture and Precipitation. *Science (80-.).* **305**, 1138–1140 (2004).

69 Seneviratne, S. I. *et al.* Investigating soil moisture-climate interactions in a changing climate: A review. *Earth-Science Rev.* **99**, 125–161 (2010).

70 Teuling, A. J. *et al.* A regional perspective on trends in continental evaporation. *Geophys. Res. Lett.* **36**, 2404 (2009).

71 Schwingshackl, C., Hirschi, M. & Seneviratne, S. I. Quantifying Spatiotemporal Variations of Soil Moisture Control on Surface Energy Balance and Near-Surface Air Temperature. *J. Clim.* **30**, 7105–7124 (2017).

72 Schär, C. et al. The role of increasing temperature variability in European summer heatwaves. *Nat. 2004 4276972* **427**, 332–336 (2004).

73 Schär, C., Luthi, D., Beyerle, U. & Heise, E. The soil-precipitation feedback: A process study with a regional climate model. *J. Clim.* **12**, 722–741 (1999).

74 Pal, J. S. & Eltahir, E. A. B. Pathways Relating Soil Moisture Conditions to Future Summer Rainfall within a Model of the Land-Atmosphere System. *J. Clim.* **14**, 1227–1242 (2001).

75 Koster, R. D., Suarez, M. J., Higgins, R. W. & Van den Dool, H. M. Observational evidence that soil moisture variations affect precipitation. *Geophys. Res. Lett.* **30**, (2003).

76 Guo, Z. *et al.* GLACE: The Global Land-Atmosphere Coupling Experiment. Part II: Analysis. (2006).

77 Findell, K. L., Gentine, P., Lintner, B. R. & Kerr, C. Probability of afternoon precipitation in eastern United States and Mexico enhanced by high evaporation. *Nat. Geosci.* **4**, 434–439 (2011).

78 Christidis, N., Jones, G. S. & Stott, P. A. Dramatically increasing chance of extremely hot summers since the 2003 European heatwave. *Nat. Clim. Chang. 2014 51* **5**, 46–50 (2014).

79 Russo, S., Sillmann, J. & Fischer, E. M. Top ten European heatwaves since 1950 and their occurrence in the coming decades. *Environ. Res. Lett.* **10**, 124003 (2015).

80 Santanello, J. A. *et al.* Land–Atmosphere Interactions: The LoCo Perspective. *Bull. Am. Meteorol. Soc.* **27**, 3713–3730 (2018).

81 López-Moreno, J. I. *et al.* Recent temperature variability and change in the Altiplano of Bolivia and Peru. *Int. J. Climatol.* **36**, 1773–1796 (2016).

82 Teuling, A. J. A hot future for European droughts. *Nat. Clim. Chang. 2018 85* **8**, 364–365 (2018).

83 Vogel, M. M. *et al*. Regional amplification of projected changes in extreme temperatures strongly controlled by soil moisture-temperature feedbacks. *Geophys. Res. Lett.* **44**, 1511–1519 (2017).

84 Samaniego, L. *et al.* Anthropogenic warming exacerbates European soil moisture droughts. *Nat. Clim. Chang. 2018 85* **8**, 421–426 (2018).

85 García-Herrera, R., Díaz, J., Trigo, R. M., Luterbacher, J. & Fischer, E. M. A Review of the European Summer Heat Wave of 2003. *Crit. Rev. Environ. Sci. Technol.* **40**, 267–306 (2010).

86 Ogi, M., Yamazaki, K. & Tachibana, Y. The summer northern annular mode and abnormal summer weather in 2003. *Geophys. Res. Lett.* **32**, 1–4 (2005).

87 Miralles, D. G., Teuling, A. J., Van Heerwaarden, C. C. & De Arellano, J. V. G. Mega-heatwave temperatures due to combined soil desiccation and atmospheric heat accumulation. *Nat. Geosci. 2014 75* **7**, 345–349 (2014).

88 Toreti, A. *et al.* The Exceptional 2018 European Water Seesaw Calls for Action on Adaptation. *Earth's Futur.* **7**, 652–663 (2019).

89 Dirmeyer, P. A., Balsamo, G., Blyth, E. M., Morrison, R. & Cooper, H. M. Land-Atmosphere Interactions Exacerbated the Drought and Heatwave Over Northern Europe During Summer 2018. *AGU Adv.* **2**, e2020AV000283 (2021).

90 Seneviratne, S. I. et al. Weather and Climate Extreme Events in a Changing Climate. in *Climate Change 2021: The Physical Science Basis. Contribution of Working Group I to the Sixth Assessment Report of the Intergovernmental Panel on Climate Change* (eds. Masson-Delmotte, V. et al.) (Cambridge University Press, 2021).

91 Vogel, M. M., Zscheischler, J. & Seneviratne, S. I. Varying soil moisture-atmosphere feedbacks explain divergent temperature extremes and precipitation projections in central Europe. *Earth Syst. Dyn.* **9**, 1107–1125 (2018).

92 Pfister, C. Wetternachhersage 500 Jahre Klimavariationen und Naturkatastrophen (1496–1995). Haupt, Bern, Stuttgart, Wien, (1999).

93 Schorer, M. Klimaänderung Schweiz: Trockenheit in der Schweiz. in *Workshop Bericht* (ed. OcCC) 17 (OcCC, 2000).

94 Brugger, H. Statistisches Handbuch der schweizerischen Landwirtschaft. (Komissionsverlag, Verbandsdruckerei AG, 1968).

95 SNB. 40. Geschäftsbericht der Schweizerischen Nationalbank. Bern, 67 (1947).

96 Erdin, D. Das Trockenjahr 2018. *AGRISTAT Aktuell* (2018).

97 Keller, F. & Fuhrer, J. Die Landwirtschaft und der Hitzesommer 2003. *Agrar. Schweiz* **11**, 403–410 (2004).

98 Fossati, D. & Brabant, C. Die Weizenzüchtung in der Schweiz. *AgrarForschung* **10**, 447–458 (2003).

99 SBV. Statistische Erhebungen und Schätzungen auf dem Gebiete der Landwirtschaft. (Schweizerisches Bauernsekretariat, 1948).

100 SBV. Statistische Erhebungen und Schätzungen über Landwirtschaft und Ernährung (SES). *SBV* (Ed.) (2021).

101 We thank Christoph Frei of MeteoSwiss for providing consistent monthly precipitation and temperature fields for 1947, 2003, and 2018.

102 Schüepp, M., Schiesser, H. H., Huntrieser, H., Scherrer, H. U. & Schmidtke, H. The winterstorm "Vivian" of 27 February 1990: About the meteorological development, wind forces and damage situation in the forests of Switzerland. *Theor. Appl. Climatol. 1994 493* **49**, 183–200 (1994).

103 Usbeck, T. *et al.* Increasing storm damage to forests in Switzerland from 1858 to 2007. *Agric. For. Meteorol.* **150**, 47–55 (2010).

104 Müller, H. Forstliche Chronik 1947. *Schweiz. Z. Forstwes.* **99**, 438–443 (1948).

105 Heinis, F. Beobachtungen über den Einfluss der Trockenheit des Sommers 1947 auf die Vegetation im unteren Baselbiet. *Tätigkeitsber. Naturforsch. Ges. Basell.* **18**, 156–159 (1949).

106 Zoller, H. & Lüdi, W. Einige Beobachtungen über die Dürreschäden des Sommers 1947 in der Nordschweiz und am Schweizerischen Jurarand. *Ber. Geobot. Forschungsinst, Rübel* 73–85 (1949).

107 Schweizer Illustrierte. 27.08.1947

108 Keller, J. Erhebung über den Borkenkäferbefall im Jahre 1949. *Prakt. Forstwirt Schweiz* **1950**, 118–127 (1950).

109 Bütikofer, N. Historische Waldschäden in der Schweiz 1800–1960. (Historisches Institiut der Unversität Bern, 1987).

110 Brunner, I. Naturchronik für das Jahr 1947. *Jahresber. Naturforsch. Ges. Graubünden* **81**, 9–13 (1948).

111 Bavier, B. Der Waldbrand am Calanda im August/September 1943. *Schweizerische Zeitschrift für das Forstwes.* **95**, 291–298 (1944).

112 Gimmi, U., Bürgi, M. & Wohlgemuth, T. Wie oft brannte der Walliser Wald im 20. Jahrhundert? *Schweizerische Zeitschrift für Forstwes.* **155**, 437–440 (2004).

113 Wohlgemuth, T. *et al.* Früher Laubfall der Buche während der Sommertrockenheit 2018: Resistenz oder Schwächesymptom? *Schweizerische Zeitschrift für Forstwes.* **171**, 257–269 (2020).

114 Dubach, V. *et al.* Waldschutzüberblick 2020. *WSL Berichte* **107**, 1–58 (2021).

115 Jakoby, O., Lischke, H. & Wermelinger, B. Climate change alters elevational phenology patterns of the European spruce bark beetle (Ips typographus). *Glob. Chang. Biol.* **25**, 4048–4063 (2019).

116 Haag, E. Die Wiederherstellung der käfergeschädigten Waldungen der ersten Jurakette ob dem Bielersee. *Schweizerische Zeitschrift für Forstwes.* **112**, 693–699 (1961).

117 Baltensweiler, A. *et al.* Räumliche Analyse von Trockenheitssymptomen im Schweizer Wald mit Sentinel-2-Satellitendaten. *Schweizerische Zeitschrift für Forstwes.* **171**, 298–301 (2020).

118 Pfister, C., Bütikofer, N., Schuler, A. & Volz, R. Witterungsextreme und Waldschäden in der Schweiz. Eine historisch-kritische Untersuchung von Schadenmeldungen aus schweizerischen Wäldern in ihrer Beziehung zur Klimabelastung, insbesondere durch sommerliche Dürreperioden. (1988).

119 BAFU. Medienmitteilung: Winterstürme Anfang 2018: Rund 1.3 Mio m^3 Holz liegen am Boden. 18.01.2018

[120] Usbeck, T. Wintersturmschäden im Schweizer Wald von 1865 bis 2014. *Schweizerische Zeitschrift für Forstwes.* **166**, 184–190 (2015).

[121] Brändli, U. B., Abegg, M. & Allgaier Leuch, B. Schweizerisches Landesforstinventar. Ergebnisse der vierten Erhebung 2009–2017. Eidgenössische Forschungsanstalt für Wald, Schnee und Landschaft WSL, Bundesamt für Umwelt BAFU, Birmensdorf, Bern (2020).

[122] Bürgi, M. & Schuler, A. Driving forces of forest management – an analysis of regeneration practices in the forests of the Swiss Central Plateau during the 19th and 20th century. *For. Ecol. Manage.* **176**, 173–183 (2003).

[123] Nagel, J.-L. Influences des éléments météorologiques sur l'accroissement des forêts. *Schweizerische Zeitschrift für Forstwes.* **101**, 512–530 (1950).

[124] WGMS. Global Glacier Change Bulletin No. 4 (2018–2019). (ISC(WDS)/IUGG(IACS)/UNEP/UNESCO/WMO, World Glacier Monitoring Service, Zürich, 2021).

[125] Steiner, D. *et al.* Sensitivity of European glaciers to precipitation and temperature – two case studies. *Clim. Chang.* **90**, 413–441 (2008).

[126] GLAMOS (1881–2021). The Swiss Glaciers 1880–2018/19, Glaciological Reports No 1–140. Yearbooks of the Cryospheric Commission of the Swiss Academy of Sciences (SCNAT), published since 1964 by VAW / ETH Zurich.

[127] Zumbühl, H. J., Nussbaumer, S. U., Holzhauser, H. & Wolf, R. Die Grindelwaldgletscher – Kunst und Wissenschaft. (Bern: Haupt, 2016).

[128] Haefeli, R. & Kasser, P. Beobachtungen im Firn- und Ablationsgebiet des grossen Aletschgletschers. *Schweizerische Bauzeitung* **66**, 489–494 (1948).

[129] Huss, M. Extrapolating glacier mass balance to the mountain-range scale: the European Alps 1900–2100. *Cryosph.* **6**, 713–727 (2012).

[130] Hoinkes, H. C. Glacier variation and weather. *J. Glaciol.* **7**, 3–19 (1968).

[131] Brönnimann, S. *et al.* Last phase of the Little Ice Age forced by volcanic eruptions. *Nat. Geosci.* **12**, 650–656 (2019).

[132] Huss, M. & Hock, R. Global-scale hydrological response to future glacier mass loss. *Nat. Clim. Chang.* **8**, 135–140 (2018).

[133] Klebelsberg, R. Die Gletscher der österreichischen Alpen 1947–1949. Bericht über die Gletschermessungen des Österreichischen Alpenvereins. *Zeitschrift für Gletscherkd. und Glazialgeol.* **1**, 203–219 (1950).

[134] Ragettli, M. S., Vicedo-Cabrera, A. M., Schindler, C. & Röösli, M. Exploring the association between heat and mortality in Switzerland between 1995 and 2013. *Environ. Res.* **158**, 703–709 (2017).

[135] Ragettli, M. S., Vicedo-Cabrera, A. M., Flückiger, B. & Röösli, M. Impact of the warm summer 2015 on emergency hospital admissions in Switzerland. *Environ. Health* **18**, (2019).

[136] Vicedo-Cabrera, A. M., Ragettli, M. S., Schindler, C. & Röösli, M. Excess mortality during the warm summer of 2015 in Switzerland. *Swiss Med. Wkly.* **146**, w14379 (2016).

[137] Grize, L., Huss, A., Thommen, O., Schindler, C. & Braun-Fahrländer, C. Heat wave 2003 and mortality in Switzerland. *Swiss Med. Wkly.* **135**, 200–205 (2005).

[138] Vicedo-Cabrera, A. M. et al. A multi-country analysis on potential adaptive mechanisms to cold and heat in a changing climate. *Environ. Int.* **111**, 239–246 (2018).

[139] Preston, S. H., Keyfitz, N. & Schoen, R. Causes of death: life tables for national population. (Seminar Press, 1972).

[140] Kueh, M. T. & Lin, C. Y. The 2018 summer heatwaves over northwestern Europe and its extended-range prediction. *Sci. Reports 2020 101* **10**, 1–18 (2020).

[141] Ragettli, M. S. & Röösli, M. Heat-health action plans to prevent heat-related deaths – experiences from Switzerland. *Bundesgesundheitsblatt - Gesundheitsforsch. - Gesundheitsschutz* **62**, 605–611 (2019).

[142] Sera, F. *et al.* How urban characteristics affect vulnerability to heat and cold: a multi-country analysis. *Int. J. Epidemiol.* **48**, 1101–1112 (2019).

[143] Romanello, M. *et al.* The 2021 report of the Lancet Countdown on health and climate change: code red for a healthy future. *Lancet* **398**, 1619–1662 (2021).

[144] Zhao, Q. et al. Global, regional, and national burden of mortality associated with non-optimal ambient temperatures from 2000 to 2019: a three-stage modelling study. *Lancet. Planet. Heal.* **5**, e415–e425 (2021).

[145] Green, H. *et al.* Impact of heat on mortality and morbidity in low and middle income countries: A review of the epidemiological evidence and considerations for future research. *Environ. Res.* **171**, 80–91 (2019).

[146] Vicedo-Cabrera, A. M. *et al.* The burden of heat-related mortality attributable to recent human-induced climate change. *Nat. Clim. Chang.* **11**, 492–500 (2021).

[147] Gasparrini, A. *et al.* Projections of temperature-related excess mortality under climate change scenarios. *Lancet. Planet. Heal.* **1**, e360 (2017).

[148] IPCC (2021) Summary for Policymakers. In: *Climate Change 2021: The Physical Science Basis. Contribution of Working Group I to the Sixth Assessment Report of the Intergovernmental Panel on Climate Change* [Masson-Delmotte, V., P. Zhai, A. Pirani, S. L. Connors, C. Péan, S. Berger, N. Caud, Y. Chen, L. Goldfarb, M. I. Gomis, M. Huang, K. Leitzell, E. Lonnoy, J.B.R. Matthews, T. K. Maycock, T. Waterfield, O. Yelekçi, R. Yu and B. Zhou (eds.)]. Cambridge University Press. In Press.

[149] climateactiontracker.org. Available at: *https://climateactiontracker.org/global/cat-thermometer*.

[150] Giorgi, F. Thirty Years of Regional Climate Modeling: Where Are We and Where Are We Going next? *J. Geophys. Res. Atmos.* **124**, 5696–5723 (2019).

[151] Kotlarski, S. *et al.* Regional climate modeling on European scales: A joint standard evaluation of the EURO-CORDEX RCM ensemble. *Geosci. Model Dev.* **7**, 1297–1333 (2014).

[152] Jacob, D. *et al.* Regional climate downscaling over Europe: perspectives from the EURO-CORDEX community. *Reg. Environ. Chang.* **20**, 1–20 (2020).

[153] Brogli, R., Kröner, N., Sørland, S. L., Lüthi, D. & Schär, C. The Role of Hadley Circulation and Lapse-Rate Changes for the Future European Summer Climate. *J. Clim.* **32**, 385–404 (2019).

[154] Kröner, N. *et al.* Separating climate change signals into thermodynamic, lapse-rate and circulation effects: theory and application to the European summer climate. *Clim. Dyn.* **48**, 3425–3440 (2017).

[155] Klimaszenarien Schweiz. Available at: *www.klimaszenarien.ch*.

[156] Schweizerische Eidgenossenschaft. Anpassung an den Klimawandel in der Schweiz: Aktionsplan 2020–2025, Bern, 164 (2020).

[157] Feigenwinter Iris *et al.* Exploring quantile mapping as a tool to produce user tailored climate scenarios for Switzerland – MeteoSwiss. (2018).

[158] Mastai, A. Storylines of future climate extremes in Switzerland. (Master's Thesis ETH Zurich/MeteoSwiss, 2022).

Photo credits

Cover (top): Private archive, Deacon Pascal Huguenin

Cover (bottom): Keystone, Anthony Anex

Fig. 1.1: Keystone, Anthony Anex

Fig. 1.3: Schweizer Illustrierte, August 27, 1947, courtesy of Ringier Axel Springer publishing house

Fig. 1.4: Private archive, Deacon Pascal Huguenin

Fig. 7.1: Schweizer Illustrierte, August 27, 1947, courtesy of Ringier Axel Springer publishing house

Fig. 7.2: Photo Ulrich Wasem

Fig. 7.3: Winterthur Libraries, Winterthur Collection

Fig. 8.4: Photo Paul-L Mercanton, Les variations périodiques des glaciers des Alpes suisses. Soixante-huitième rapport – 1947. *Les Alpes* **24**, 8 (1948)

Fig. 9.2: ETH-Bibliothek Zurich, picture archive / Photographer: Comet Photo AG (Zurich) / Com_M01-0455-0006 / CC BY-SA 4.0

Fig. 10.6: Peeradontax/Shutterstock.com

GEOGRAPHICA BERNENSIA

Open Access Online Publications

www.geography.unibe.ch/services/geographica_bernensia/online_publications/

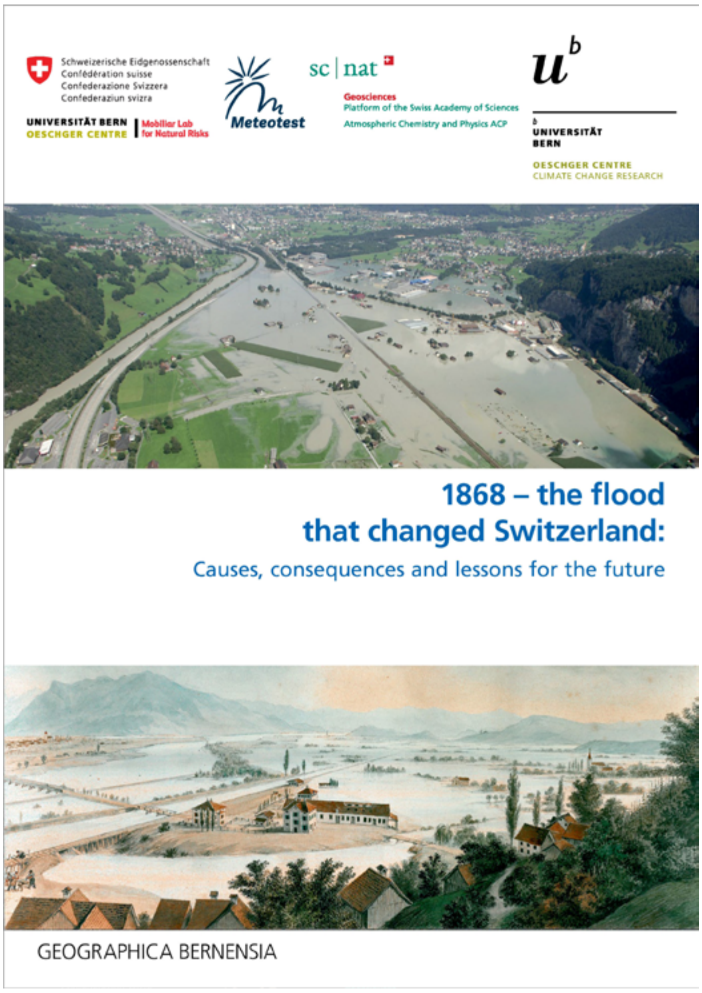

Brönnimann, S.; Rohr, C.; Stucki, P.; Summermatter, S.; Bandhauer, M.; Barton, Y.; Fischer, A.; Froidevaux, P. A.; Germann, U.; Grosjean, M.; Hupfer, F.; Ingold, K. M.; Isotta, F.; Keiler, M.; Romppainen-Martius, O.; Messmer, M. B.; Mülchi, R. I.; Panziera, L.; Pfister, L. M.; Raible, C.; Reist, T.; Rössler, O.; Röthlisberger, V.; Scherrer, S. C.; Weingartner, R.; Zappa, M.; Zimmermann, M.; Zischg A. (2018) 1868 – the flood that changed Switzerland: Causes, consequences and lessons for the future. Geographica Bernensia G94, 51 S., doi:10.4480/GB2018.G94.04

Rutishauser, T.; Brönnimann, S.; Gehrig, R.; Pietragalla, B.; Baumgarten, F.; Vitasse, Y.; Stöckli, S.; Pfister, C.; Holzkämper, A.; Hund, A.; Fossati, D.; Meier, M.; Weingartner, R.; Buchmann, M. (2020) Klimawandel und Jahreszeiten. Geographica Bernensia G97, 27 S., doi:10.4480/GB2020.G97.01